

NORTHWESTERN UNIVERSITY

Defining the role of Ikaros as a tumor suppressor and repressor of Notch target genes

A DISSERTATION

SUBMITTED TO THE GRADUATE SCHOOL
IN PARTIAL FULFILLMENT OF THE
REQUIREMENTS

For the degree

DOCTOR OF PHILOSOPHY

Field of Integrated Graduate Program in the Life Sciences

By

Katie L Kathrein

EVANSTON, ILLINOIS

June 2008

Abstract

Defining the role of Ikaros as a tumor suppressor and repressor of Notch target gene expression

Katie L Kathrein

Inactivation of tumor suppressors genes, which encode regulatory proteins critical for maintaining normal cellular function, is a common occurrence in cancer. Ikaros is a hematopoietic-specific zinc finger protein that functions as a differentiation regulator and has properties of a tumor suppressor. Ikaros functions to regulate gene expression as a component of chromatin remodeling complexes, which serve to maintain and alter the accessibility of DNA, thereby facilitating or preventing gene expression. Ikaros null mice develop T cell leukemia with 100% entrance and deregulation of Ikaros expression has been observed in some forms of human leukemia, including acute lymphoblastic leukemia (ALL) and chronic myelocytic leukemia (CML).

Using an *ex vivo* retroviral transduction system to restore Ikaros activity to an Ikaros null leukemia T cell line, JE131, we show that expression of Ikaros causes growth arrest at the G0/G1 phase of the cell cycle, an increase in expression of p27Kip1 and induction of T cell differentiation markers, such as CD4 and CD8. Restoration of Ikaros activity also results in a global increase in histone acetylation on histone H3.

Our work has also focused on defining the interaction between Ikaros and Notch, which is also commonly deregulated in human leukemia, using the JE131 model system. We show that cleaved Notch1, intracellular notch (ICN), is expressed aberrantly in the JE131 Ikaros null T cell

line. However, addition of γ -secretase inhibitors, which prevents cleavage of the Notch1 receptor to generate ICN, fails to potently inhibit growth. This demonstrates that loss of Ikaros alone, not expression of a Notch oncogene, is required for the aberrant growth observed in Ikaros null cells. We have identified a Notch1 target gene, Hairy and enhancer of split homolog-1 (Hes1) as a potential target of Ikaros' repressive activity. It is expressed at high levels in JE131 cells, but is rapidly downregulated upon restoration of Ikaros expression. Using chromatin immunoprecipitation, Ikaros is shown binding directly to the Hes1 promoter. Our work suggests that Ikaros functions as a tumor suppressor in part through regulation of Notch target gene expression.

Acknowledgements

Thank you to Susan Winandy for her thoughtful guidance and role as a teacher, mentor and friend throughout my graduate school experience. Also, thank you to the members of the Winandy lab: Ben Brugmann, Sheila Chari, Erin Griffiths, Jenny Lehman, Rachelle Lorenz, Angela Minniti Innes, Sarah Umetsu, Julie Urban and Heather Wojcik. You all have helped support me, serving as references for ideas and discussion.

Table of Contents

| | |
|---|-----------|
| I. Introduction | 7 |
| Cancer and cancer development | 7 |
| Leukemia | 9 |
| Ikaros | 9 |
| Ikaros and leukemia | 12 |
| Ikaros and chromatin remodeling | 13 |
| Ikaros as a classic transcription factor | 16 |
| Post-translational regulation of Ikaros activity | 17 |
| T cell development | 19 |
| Chromatin remodeling in T cell development | 20 |
| Ikaros and T cell development | 21 |
| Notch | 23 |
| II. Materials and Methods | 27 |
| Cell lines and cell culture | 27 |
| Protein preparation and immunoblotting | 27 |
| Retroviral constructs | 29 |
| Retroviral transduction | 30 |
| Cell sorting | 30 |
| Antibodies | 31 |
| Cell staining and flow cytometry | 31 |
| RT-PCR | 32 |
| Cell cycle analysis and Pyronin Y staining | 33 |
| Chromatin immunoprecipitation | 34 |
| Chromatin immunoprecipitation Western blot | 35 |
| III. Ikaros induces quiescence and T cell differentiation in JE131 cells | 36 |
| Results | 37 |
| Discussion | 59 |
| IV. Ikaros directly represses the Notch target gene <i>Hes1</i> in JE131 cells | 63 |
| Results | 65 |
| Discussion | 86 |
| V. Summary | 93 |
| References | 95 |

Figures

| | |
|---|----|
| 1. Schematic representation of Ikaros isoforms | 11 |
| 2. Functional and interaction domains of the Ikaros protein | 18 |
| 3. Notch Pathway Model | 24 |
| 4. Phoenix cell retroviral transduction system | 40 |
| 5. Retroviral expression levels of Ik-1 are comparable to expression levels of DNA binding Ikaros isoforms in wild-type mouse | 41 |
| 6. Reintroduction of Ikaros into the JE131 cells has a profound effect on their growth properties | 42 |
| 7. Reintroduction of Ikaros to JE131 cells results in loss of H-2K ^k and Ikaros expression after 5 days in culture | 44 |
| 8. Appearance of a “small cell” population in Ik-1 expressing JE131 cells | 45 |
| 9. “Small cell” population of Ik-1 expressing cells are arrested G0/G1 | 47 |
| 10. Percent of cells undergoing apoptosis is equal among transduced JE131 cells | 50 |
| 11. Ik-1 transduced JE131 cells display an increase in p27kip1 expression | 52 |
| 12. Growth of JE131 cells can be slowed by retroviral transduction of p27kip1 | 54 |
| 13. Reintroduction of Ik-1 into JE131 cells induces a T cell differentiation program | 56 |
| 14. Expression of Ik-1 in JE131 cells induces widespread changes in histone acetylation | 58 |
| 15. Expression of the Notch target gene, <i>Hes1</i> , is repressed upon reintroduction of Ik-1 to JE131 cells | 66 |
| 16. JE131 cells contain intracellular Notch | 68 |
| 17. The γ -secretase inhibitor, DAPT, has minimal effects on growth of JE131 cells, but leads to upregulation of CD4 | 69 |
| 18. Preventing downregulation of <i>Hes1</i> decreases Ikaros’ ability to induce high-level expression of CD4 | 73 |
| 19. DNA binding specificity is required for Ikaros’ ability to repress <i>Hes1</i> | 76 |
| 20. Ikaros and RBP-J κ bind to the regulatory region on <i>Hes1</i> | 79 |
| 21. Ikaros and RBP-J κ bind to the regulatory regions of <i>Deltex1</i> | 88 |
| 22. Two hypotheses for cooperative DNA binding of Ikaros and RBP-J κ during gene repression | 89 |

Chapter I

Introduction

Cancer and cancer development

Disruption in signaling, differentiation, apoptosis, and/or proliferation in cells can lead to the deregulation of normal cell functions and the formation of cancer. Understanding the mechanisms and consequences of these deregulations is critical to treatment and prevention. Oncogenes and tumor suppressor genes are often targets of deregulation in cancer. Genetic alterations modify the function of these genes, often resulting in transformation. The genetic alterations causing transformation have been shown to occur by a “two hit” method for tumor suppressors, where both copies of the gene must be mutated to cause disease (1). These genetic abnormalities can be inherited or caused by an external source, such as carcinogen exposure. Only one hit is necessary for oncogenes (2).

Oncogenes, which are termed proto-oncogenes prior to mutation and transformation, are genes that, when altered by gain of function, can cause the development of tumors. Proto-oncogenes are widespread in the genome, functioning normally to regulate many different cell functions, including proliferation, apoptosis, gene stability and differentiation (3). Myc is an example of a well-characterized proto-oncogene that is often aberrantly expressed in tumors (4). Overexpression of this transcription factor in cells promotes proliferation (5) and inhibits cell differentiation (6).

Tumor suppressor genes differ from oncogenes in that loss of function of these genes, rather than gain of function, contributes to transformation. Tumor suppressors are also found throughout the genome, regulating normal cellular functions such as proliferation, apoptosis, and

differentiation. Inactivation of tumor suppressors increases the potential for neoplasia, while restoration of their function can restore some of the altered functions (3). There are also many well-characterized tumor suppressor genes. Mutation of the tumor suppressor p53 is the most common mutation found in cancer, occurring in more than 50% of primary tumors (7). p53 is a DNA binding protein that functions to prevent aberrantly growing cells from progressing by halting the cell cycle and promoting apoptosis. DNA damage activates p53, arresting the cell cycle at the G1 phase (8). Thus, loss of p53 allows potentially damaged cells to survive and expand. The importance of p53 expression has been demonstrated in experiments reintroducing expression to cells that lack p53 expression. p53 null glioblastoma and osteosarcoma cells lines with forced p53 overexpression demonstrate reduced growth potential (9, 10). Reintroduction of p53 into a T cell lymphoma line results in upregulation of the cell cycle inhibitor, p21 contributing to cell cycle arrest (11). Growth arrest is associated with apoptosis upon reintroduction of p53 in a p53 null myeloid leukemia cell line (12). Apoptosis resulting from p53 expression may occur through transcriptional repression of the anti-apoptotic factor BCL-2 (13). Reintroduction of p53 can also promote differentiation, as shown in several leukemia lines (14, 15).

WT1 is another tumor suppressor whose normal function is important for cell growth and differentiation. WT1 is a zinc finger transcription factor whose transcriptional targets include genes important for growth, transcription, and formation of the extracellular matrix (16-18). Growth control and/or arrest are observed in WT1 null cell lines upon transduction with wild type WT1 (19, 20). Retroviral reintroduction of WT1 to myeloid leukemia cell lines led to cell cycle arrest and differentiation (21). In contrast to other tumor suppressors, however, WT1 has

been shown to have oncogenic potential in some cancers. In leukemia, overexpression of WT1 is often observed in patient samples and is associated with poor disease prognosis (22).

Leukemia

Leukemia is tumor formation in the hematopoietic compartment. Like other cancers, the origins of leukemia often involve mutations in proto-oncogenes and tumor suppressors. These mutations can occur at any of the different stages of hematopoietic development and results in aberrant expansion of tumor cells in bone marrow, blood, or lymphoid tissues. Acute leukemia consists of rapidly growing, immature blasts, as opposed to chronic leukemia, which consists of few or no blasts. There are two types of acute leukemia, acute myelogenous leukemia (AML), leukemia of the myeloid lineage and acute lymphocytic leukemia (ALL), leukemia of lymphoid cells. In AML, mutations in Runx1 (AML1) transcription factor are common and frequently result from a translocation of genes that disrupt the normal function of the Runx1 and/or the other genetic component of the translocation (23). There are two subsets of ALL, those of either B cell or T cell origin. T cell derived ALL, or T-ALL, arises from cells that have committed to T cell fate and is the most common cancer in children. Oncogenes and tumor suppressors play important roles in T-ALL, as in other cancers. Mutations in the transcription factor Ikaros have been identified in leukemia and suggest it may function as a tumor suppressor.

Ikaros

Ikaros is an almost exclusively hematopoietic specific DNA binding transcription factor that has been shown to be important for proper T cell development, homeostasis and has

characteristics of a tumor suppressor. Ikaros was discovered in a screening for a master regulator of T cell development. The enhancer sequence of the CD3 δ gene, one of the earliest T cell differentiation markers, was used as bait for a T cell expression library, which identified Ikaros (24).

The Ikaros gene encodes at least six different isoforms of the Ikaros protein, Ik-1 through 6 (**Figure 1**). The isoforms vary in expression through embryogenesis, but Ik-1, and Ik-2 are consistently the most abundantly expressed isoforms. However, at mid-gestation, levels of Ik-1, Ik-2 and Ik-4 are nearly equivalent. This is not the result of increased Ik-4 expression, but rather a reduction in Ik-1 and Ik-2 expression. Ik-3 and Ik-5 are also detectable during development, but expression levels were very low (25). In adults, Ikaros is expressed in progenitor and mature T cells and early and mature B cells (24).

Ikaros isoforms differ in their exonic structure formed through alternative splicing. All isoforms contain exons 1,2 and 7. Exon 7 encodes two C-terminal zinc fingers (F5 and F6), which allow Ikaros to oligomerize with other Ikaros proteins and Ikaros family member proteins (26). Exons 3, 4 and 5 encode four N-terminal zinc fingers, which function to directly bind the DNA consensus sequence GGGAA, shown through electromobility shift assays (EMSA) (25). All Ikaros zinc fingers' structure is consistent with the Kruppel Cys-2 His-2 motif (27) and requires binding of a zinc ion for proper function (26, 28). Ik-1 contains all of the possible exons, which encode all four N-terminal zinc fingers, F1-F4. Ik-2 and Ik-3 lack internal exons, but retain at least three zinc fingers. Ik-4, Ik-5 and Ik-6 all contain two or fewer zinc fingers (25, 28).

The differences in N-terminal zinc finger content have important implications for the

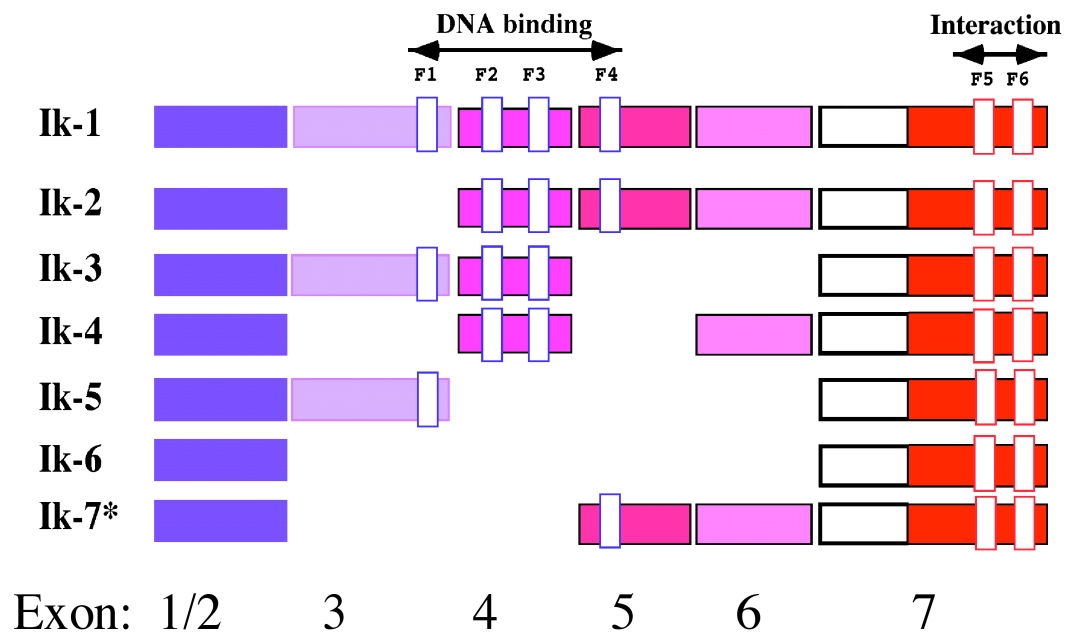


Figure 1. Schematic representation of Ikaros isoforms. Zinc finger domains involved in DNA binding (F1-F4) and protein interaction (F5 and F6) are indicated by arrows. Star denotes the mutant dominant negative isoform (Ik-7).

functions of the different Ikaros isoforms because Ikaros binds DNA through these zinc fingers (25, 28). DNA binding by Ikaros requires at least three zinc fingers (26), so only isoforms Ik-1, Ik-2, and Ik-3 have sufficient zinc fingers for this function. Isoforms Ik-4, Ik-5 and Ik-6 do not have strong affinity for DNA (25, 28). Because Ikaros isoforms can oligomerize, the non-DNA binding isoforms lower the affinity of the entire complex for DNA, rendering it unable to bind DNA (26). Thus, non-DNA binding isoforms act in a dominant negative fashion on DNA binding competent isoforms. This characteristic has important consequences in leukemia.

Ikaros and Leukemia

The non-DNA binding isoforms of Ikaros, which are normally expressed at low levels, are often found at high levels in primary leukemic cells from patients (29-31). The consequence of high expression of non-DNA binding isoforms is believed to result in a decrease of Ikaros function through the dominant negative phenotype. Dominant negative Ikaros activity is hypothesized to accelerate disease by preventing Ikaros from functioning as a DNA binding transcription factor. The abundance of Ikaros mutations suggests that inactivation of Ikaros function is advantageous to transformation.

The human Ikaros gene is 95% homologous to the mouse Ikaros gene (32) and leukemic development is witnessed in mice with Ikaros mutations. Mice that are homozygous null for Ikaros, through a disruption in exon 7, develop leukemia with 100% penetrance within 6 weeks from birth (32-34). Similar to the disease observed in humans, expression of a dominant negative, non DNA-binding isoform also results in leukemia (34), further emphasizing the

importance of appropriate Ikaros expression in prevention of leukemia. These data also suggest that Ikaros acts as a tumor suppressor.

Ikaros and Chromatin Remodeling

The development of leukemia in mice with Ikaros mutations suggests that Ikaros is important for maintaining proper development and homeostasis in normal cells and that deletion or mutation of Ikaros can result in leukemogenesis. One function of Ikaros that may contribute to its role in tumor suppression is the ability to interact with chromatin remodeling complexes (26).

Chromatin consists of highly folded and compacted complexes of DNA and proteins. Nucleosomes are the individual units of chromatin, where two turns of DNA (146 base pairs) are wrapped around an octamer of histones consisting of an H3-H4 tetramer and two H2A-H2B dimers. Histones are small proteins containing a globular domain and a protruding NH₂ terminus, forming the histone tail. Post-translational modifications of histones include addition and removal of acetyl, phosphate and methyl groups and ubiquitination (35). Addition and removal of these molecules on individual histones can alter overall chromatin conformation.

Ikaros has been shown to interact with chromatin remodeling complexes that modify histones through acetylation, deacetylation and nucleosome remodeling. The enzymatic activity required for acetylation of histones is supplied by histone acetylases (HATs). These enzymes facilitate the addition of acetyl groups to histone tail, which can lead to an open chromatin conformation, where transcription factors can interact with DNA allowing for transcription. Histone deacetylases (HDACs) facilitate the removal of acetyl groups from histones, leading to

closed conformation of DNA, hindering transcriptional regulators from interacting with DNA. Nucleosome remodeling is facilitated by enzymes with helicase/ATPase activity.

Control of histone modification status is achieved through the activities of multi-subunit chromatin remodeling complexes. Ikaros has been shown to interact with different complexes associated with chromatin remodeling, including the NuRD and SWI/SNF complexes (26). The two associated complexes are involved in closing and opening of nucleosomes, respectively, suggesting that Ikaros can both activate and suppress gene expression through the modification of nucleosome conformation (26, 36-38).

The NuRD complex, or nucleosome remodeling and deacetylase complex, is a 2MDa multi-subunit complex that contains three important enzymatic components, two HDACs and Mi-2 (39, 40). Mi-2, which contains a DNA helicase/ATPase domain, functions in ATP dependent nucleosome remodeling (40, 41), complementing the deacetylase activity of the two HDACs. Another component, the metastasis associated protein (MTA), contains a zinc finger domain and has been shown to be essential for formation of the deacetylase complex (40). The NuRD complex serves to make DNA inaccessible to transcription factors and can maintain an inaccessible, closed conformation of DNA (36).

Ikaros has been shown to associate with the NuRD complex in activated T cells through colocalization studies, where Ikaros and HDAC and Ikaros and Mi-2 were shown to overlay in toroidal structures (37). These data were confirmed with co-immunoprecipitations, which showed an association between Ikaros and components of the NuRD complex. Deletion of the F4 zinc finger severely impaired Ikaros' ability to interact with Mi-2, suggesting that zinc finger structure may play a role in Mi-2 interaction (42).

In addition, Ikaros has been shown to co-localize with the SWI/SNF complex. This multi-subunit complex is associated with nucleosome remodeling through the activity of a helicase/ATPase supplied by either Brm or Brg-1 (43). It is believed that SWI/SNF activity facilitates opening of DNA for gene expression through the activity of Brm/Brg-1 (44). An association between Ikaros and Brg-1 was observed in resting cells, co-localized in discrete, punctate structures dispersed throughout the nucleus. These data were confirmed by co-immunoprecipitation (37).

Ikaros has also been found to associate with Sin3. Sin3 a component of another large, multi-subunit chromatin remodeling complex that, like NuRD, localizes with HDACs and is responsible for repression of gene expression (45). Sin3/HDAC shares function and subunits with NuRD however, Sin3/HDAC mediated repression is thought to be more transient than that mediated by the NuRD complex (46). In a yeast two-hybrid assay using the C-terminus of Ikaros as bait, Sin3 was identified interacting with Ikaros. This association was confirmed in primary T cells (38). Deletion of the F4 zinc finger or the C-terminal portion of Ikaros impaired Ikaros-Sin3 mediated repression, suggesting that the F4 zinc finger is also critical for Sin3 mediated repression (46).

Finally, Ikaros has been shown to interact with the C-terminal binding protein (CtBP). CtBP is a transcriptional co-repressor that can recruit HDACs in a sequence specific manner to facilitate gene repression. The CtBP binding motif, PXDLS, has been found in class II HDACs (47). This motif, however, is not essential for CtBP interactions, as HDAC1 associated with CtBP, but lacks the binding motif (48). A CtBP binding motif (PEDLS) was uncovered in the 5'

region of Ikaros and further testing revealed that Ikaros interacts with CtBP *in vitro* and *in vivo* (49). Mutation of the CtBP binding site in Ikaros prevented Ikaros and CtBP interactions (49).

The ability of Ikaros to interact with multiple distinct chromatin remodeling complexes provides strong evidence that Ikaros may be responsible for broad regulation of gene expression through chromatin remodeling of target genes, functioning as both a repressor and an activator. It is hypothesized that Ikaros performs by targeting the chromatin remodeling complexes to specific gene loci, allowing for either expression or repression of the target gene, depending on the associated complex.

Ikaros as a classic transcription factor

Ikaros has been shown to function as a more traditional transcription factor through transcriptional activation and repression assays. In NIH3T3 cells, Ik-1 induced expression of a reporter gene downstream of four Ikaros binding sites, but when expressed with the non-DNA binding isoforms, reporter gene expression was significantly reduced (26). The transcriptional activation domain was mapped to a region upstream of the C-terminal zinc fingers in exon 7 through tethering of Ikaros domains to a heterologous DNA binding domain in a yeast one-hybrid assay (26). However, in the context of full length Ikaros, the defined activation domain was not found to be necessary for transcriptional activation by Ikaros in NIH3T3 cells (46), suggesting that conformational changes may be required to expose the domain or that it does not function as originally discovered.

Ikaros was also shown to function as a transcriptional repressor through fusion with a heterologous DNA binding domain in NIH 3T3 cells. Even non-DNA binding isoforms

repressed activity of the reporter gene. The domains responsible for repression were mapped to two regions within the Ikaros protein, one in the N-terminal portion, and the other in the C-terminal portion (42) (**Figure 2**). These data demonstrate the complexity of Ikaros function and suggest that Ikaros may function through multiple pathways to maintain homeostasis and prevent leukemia.

Post-translational regulation of Ikaros activity

Regulation of Ikaros activity is a relatively unstudied field. However, existing data has interesting implications for Ikaros function. Post-translational modification of Ikaros was recently shown to regulate Ikaros mediated cell cycle arrest at the G1/S transition when Ikaros was ectopically expressed in NIH3T3 cells. In these studies, Ikaros was shown to have phosphorylation sites that regulate this activity. Phosphorylation was shown to inhibit Ikaros' ability to negatively regulate cell cycle progression. The inhibition was revealed to occur because phosphorylation reduced the affinity of Ikaros for DNA (50). This form of regulation of DNA binding zinc fingers was confirmed in studies with artificial zinc finger proteins, which showed that phosphorylation decreased affinity for DNA in the four tested proteins (51). These data represent an important mechanism for Ikaros regulation that reduces Ikaros activity in a manner other than by expression of dominant negative isoforms.

In addition, recent data has shown that Ikaros can be post-translationally modified by sumoylation. This modification impairs Ikaros mediated transcriptional repression when tethered to a heterologous DNA binding domain. Sumoylation occurs on two lysine residues, 58 and 240, in the Ikaros protein. Mutation of either sumoylation site relieves the negative effect on

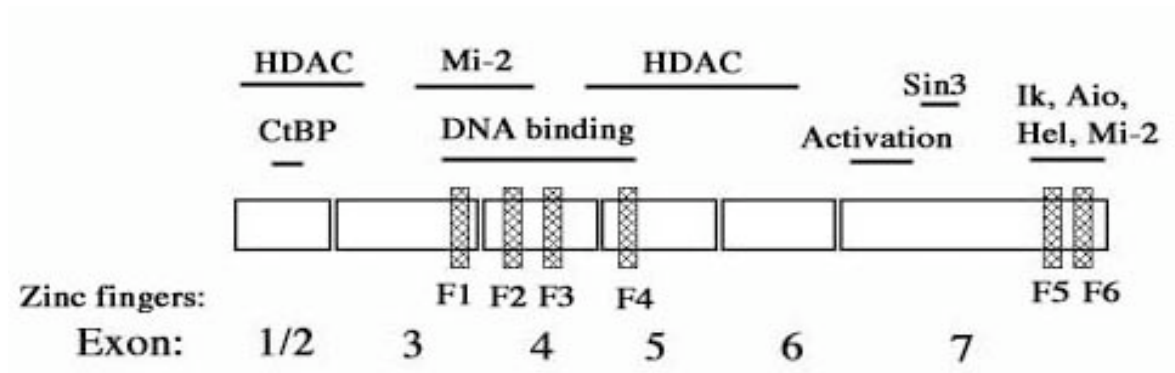


Figure 2. Functional and interaction domains of Ikaros protein. Zinc fingers are denoted by rectangular boxes in exons 3, 4, 5 and 7 (F1-F6).

transcriptional repression, thus indicating that both sites must be sumoylated to alter Ikaros' function. Sumoylation disrupts Ikaros interaction with Mi-2, CtBP and Sin3 (52). These data demonstrate cellular mechanisms important in regulating Ikaros activity, which could also potentially affect homeostasis and tumor suppression.

T cell development

Development of T cells is a multi-step process that begins with migration of T cell progenitors from the bone marrow to the thymus. These cells begin receiving signals that direct their development (53). Thymocyte maturation is marked by expression of different surface proteins and rearrangement and surface expression of the T cell receptor (TCR). Progenitor cells entering the thymus are initially categorized at the double negative (DN) stage of development, where they express neither CD4 nor CD8. The DN phase is broken into four stages, based on expression of other surface markers, namely CD25 and CD44 (54). DN1 is characterized by expression of CD44, but no CD25. In the DN2 stage, both CD25 and CD44 expression can be detected. DN3 is characterized by downregulation of CD44. Rearrangement of the β chain of the T cell receptor (TCR β) and β selection of cells with a functional pre-TCR occur at this stage and is accompanied by a proliferation burst (55). Finally, in the DN4 stage, expression of both CD25 and CD44 ceases.

These events are followed by upregulation of CD4 and CD8, where cells enter the double positive (DP) stage of T cell development and TCR α rearrangement occurs (56). Expression of TCR is observed on the surface of cells at this stage and development relies on TCR specificity for positive and negative selection. Positive selection is mediated by interaction of TCR with

self-antigen presented by cortical thymic epithelial cells (57). It is postulated that there is a threshold of affinity for this interaction that results in the delivery of survival and differentiation signals. If the affinity/avidity is below the threshold, the cells die by apoptosis, ensuring that only DP thymocytes that can recognize antigen in the context of self-MHC develop. Expression of cell surface markers CD5 and CD69 are observed upon positive selection. Concomitant with positive selection, CD4 and CD8 lineage fate is determined by whether TCR interacts with antigen in the context of MHC class I (CD8) or MHC class II (CD4). Negative selection of thymocytes also occurs, to ensure that TCRs that interact with self-MHC/self-peptide with high affinity/avidity are eliminated by apoptosis to prevent autoimmunity. This complicated, multi-step process insures that T cells will properly recognize antigens, but not self-peptides.

Chromatin Remodeling in T cell development

Chromatin remodeling has been shown to be critical for proper T cell development. At the DN stage of T cell development, inappropriate expression of CD4 is observed in mice with a thymocyte targeted deficiency for Brg-1, the ATPase/helicase subunit of the SWI/SNF chromatin remodeling complex. In addition, CD8 expression is never activated (58), thus no DP thymocytes are observed and T cell development is blocked, which was verified in a similar model of Brg-1 deficiency (59).

Mi-2 β also plays a role in T cell development, though not through repression by the NuRD complex. Targeted deletion of Mi-2 β in thymocytes led to reduced thymic cellularity and reduced levels of CD4 expression. CD4 expression was shown to be regulated by Mi-2 β through interaction with the histone acetyltransferase, p300, and HEB, a sequence specific DNA binding

protein (60), which has been shown to regulate CD4 expression (61). Taken together, these data provide evidence that chromatin remodeling is essential for thymocyte development.

Ikaros and T cell development

Ikaros has also been shown to be important in T cell development through transgenic expression of dominant negative Ikaros or deletion of Ikaros in mice. These two strains demonstrate a critical role for Ikaros in proper lymphoid development. Ikaros-deficient mice have a targeted deletion of exon 7, the region of Ikaros that is necessary for oligomerization of Ikaros family members through zinc finger protein-protein interactions. This deletion prevents expression of stable Ikaros proteins, thus yielding a null mutation. Ikaros null mice display defects in hematopoiesis, lacking all B, NK and fetal T cells. T cells develop postnatally, however a 3-9 fold decrease in thymic cellularity is observed (33, 62). These T cells are hyperproliferative upon engagement of the TCR complex (63) and a skewing to the CD4+ T cells is observed in mature populations (64). Furthermore, transformation occurs in these cells within 6 weeks of birth (33).

Mice homozygous for a dominant negative isoform of Ikaros, where exons 3 and 4 are deleted, display a more severe phenotype than the Ikaros null mutation. These mice express a non-naturally occurring isoform of Ikaros, Ik-7 (**Figure 1**). Development of all lymphoid lineages is blocked and these mice do not survive past 3 weeks (65). Surprisingly, mice heterozygous for Ik-7 appear normal for the first few weeks. However, after this time, abnormal T cell proliferation of clonal populations are observed, developing between the third and sixth months. Clonal populations have lost the wild-type Ikaros allele and are hyperproliferative in

response to TCR signaling (63). These data show that mutations altering Ikaros expression are unfavorable to T cell development.

A specific role for Ikaros in regulation of gene expression in T cell development has been defined. Chromatin immunoprecipitation (ChIP) studies using anti-Ikaros antibodies for the immunoprecipitation have shown that Ikaros can bind regulatory regions in the *CD8 α* gene (66). These studies also showed that reduction of Ikaros levels resulted in fewer CD8⁺ SP and DP cells in mice, suggesting that Ikaros may function to positively regulate CD8 expression and that absence of Ikaros hinders CD8 expression. A role for Ikaros in CD4 expression has also been described (67). Ikaros ChIP in thymocytes revealed Ikaros binding to the silencer region of the *CD4* locus. In support of a role for Ikaros in regulation of CD4 expression, Ikaros null thymocytes at the DN4 stage of T cell development express CD4, suggesting that Ikaros is important for repression of CD4 expression at these stages.

In addition, Ikaros has been shown to interact with regulatory elements of the *terminal deoxynucleotidyl transferase* gene (*TdT*) (68). The polymerase activity of TdT facilitates addition of nucleotides to TCR genes during rearrangement (69) and is responsible for expanding the repertoire of antigenic peptides recognized by T cells. By DNase1 footprinting, Ikaros was shown to bind to the promoter region of *TdT*. Transient transfection assays with a *TdT* expression reporter gene showed that Ikaros facilitates downregulation of *TdT* expression (70). These data demonstrate that Ikaros is important for T cell development through regulation of specific gene loci.

Notch

Notch, like Ikaros, is essential for T cell development, as well as survival, proliferation and differentiation in many other cell types. Notch was first discovered in *Drosophila* as being critical for neuronal and epidermal cell differentiation (71). In humans, Notch was identified through characterizations of translocations in T-ALL (72). In these cells, Notch was identified as a component of a translocation product with the TCR β . In lymphocyte development, retroviral expression of Notch in bone marrow cells promotes progenitor cell development to the T cell lineage (53) and deletion of Notch blocks T cell development (73). Notch expression on the surface of DN thymocytes was detected through the DN4 stage, but absent in DP cells (74), indicating the importance of Notch expression for T cell development at multiple stages.

The Notch family consists of four receptors, Notch1, 2, 3, and 4 (75). Expression of Notch1, 2 and 3 is observed in T cells (76), however only Notch1 has been shown to be essential in T cell development (73). The Notch receptor is expressed on the cell surface and upon ligand binding by either Delta-like or Jagged, undergoes two cleavage events (77) (**Figure 3**). The proteolytic cleavages of the intracellular domain are mediated in part by a presenilin containing γ -secretase complex (78). This results in the formation of intracellular Notch, or ICN. ICN then translocates to the nucleus and forms an activation complex with the DNA binding factor, RBP-J κ (RBP-J) and other co-activators (79, 80). It's hypothesized that prior to ICN binding, RBP-J is bound to Notch target genes as a repressive complex in association with HDACs (81). This repressive complex has recently been shown to recruit CtBP to contribute in repression (82). Interestingly, CtBP has also been shown to interact with Ikaros. ICN binding to RBP-J displaces the repression machinery with an activating complex. RBP-J binds to DNA in a sequence

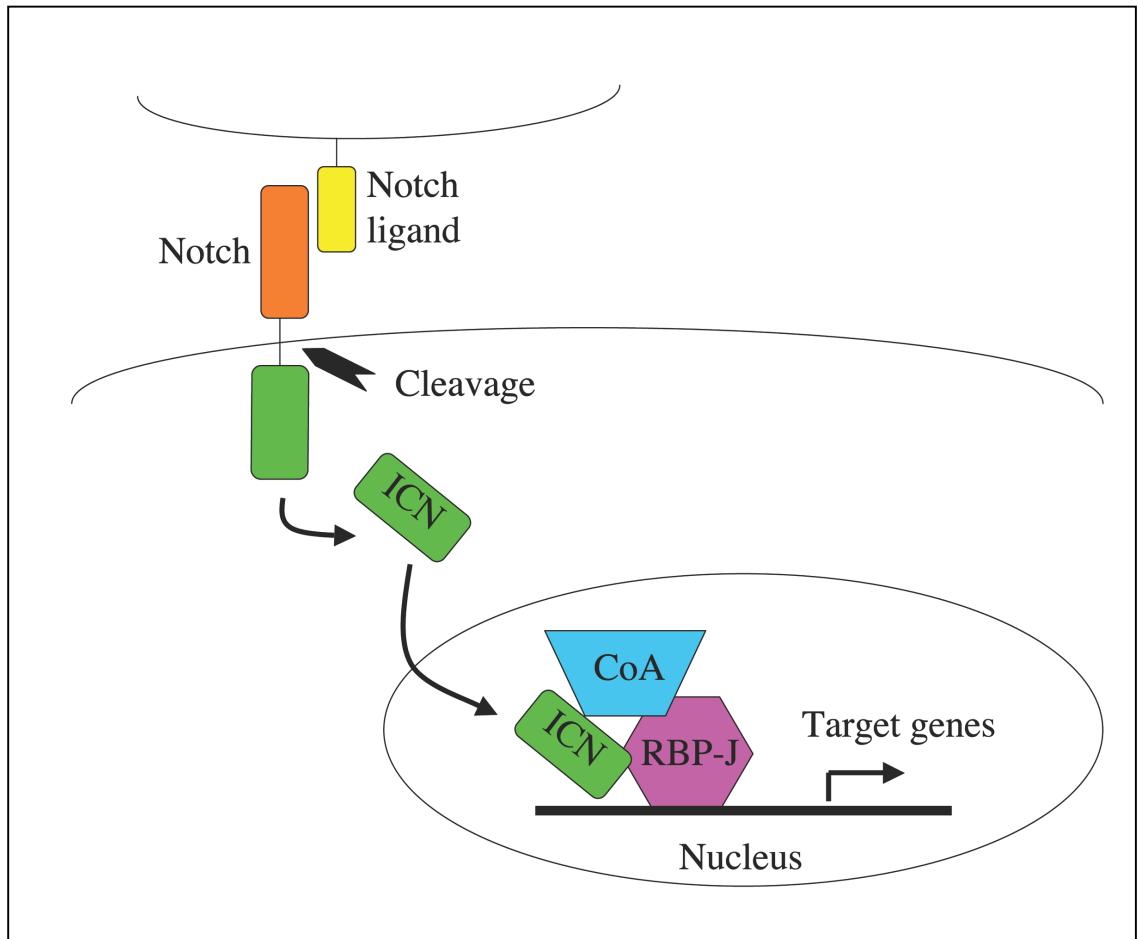


Figure 3. Notch Pathway Model. ICN: Intracellular Notch; CoA: Co-activators.

specific manner, binding to the sequence G/TGGGAA (83). Surprisingly, RBP-J shares its DNA binding consensus sequence with Ikaros (25).

Like Ikaros, only a handful of direct Notch target genes have been identified. Two of the canonical Notch target genes are *Deltex1* and *Hes1*. *Deltex1* is characterized as a Notch responsive positive transcriptional regulator though its function is not well understood (84, 85). *Hes1* or Hairy Enhancer of Split-1 (*Hes1*) is a transcription factor that, like *Notch1*, is essential for T cell development (86). Like Ikaros and Notch, targets of *Hes1* are largely unknown.

Notch deregulation has been observed in leukemia. As previously mentioned, Notch was identified in mammals through a screen of T-ALL samples. In addition, activating *Notch1* mutations are found in the majority of tested T-ALL samples (87). Unlike Ikaros, Notch functions as an oncogene, where gain of function accelerates the onset of disease. Ligand independent cleavage of Notch can occur, leading to inappropriate Notch target gene expression (88). Mutations in the C-terminal domain of Notch prevent degradation and can also be oncogenic (87). The importance of Notch in T cell development and the prevalence of Notch mutations in leukemia suggest that expression and regulation of Notch are vital for lymphocyte function.

Disease progression in Notch induced leukemia has also been shown to be accelerated by Ikaros inactivation (89, 90). In Notch induced leukemia, proviral insertional mutagenesis by murine leukemia virus in the Ikaros locus was shown to promote a more aggressive disease (89). Leukemia arising through Notch overexpression resembles that observed upon loss of Ikaros, where in both cases, leukemia is specific for the T cell lineage, arises within thymocyte population, and requires pre-TCR or TCR signaling (33, 62, 91). These data suggest a

cooperation between Ikaros and Notch for proper T cell development and prevention of leukemia.

Chapter II

Materials and Methods

Cell Lines and Cell Culture

JE131 cells were derived from the thymus of an Ikaros null mouse with spontaneous T cell leukemia. The thymus was aseptically removed and ground between two glass slides to release thymocytes. Cells were plated and within two weeks robustly proliferating cells were observed. The D510 cell line has been previously described (37). Jurkat, D0.11, D510, and JE131 cells were maintained in RPMI medium (Gibco) supplemented with 10% bovine growth serum, 50 mM β -mercaptoethanol, and 500 U/ml of penicillin-streptomycin (RPMI complete). For inhibitor assays, equal volumes of γ -secretase inhibitor DAPT [N-N-(3,5-Difluorophenacetyl)-L-alanyl-(S)-phenylglycine t-butyl ester] (Calbiochem) resuspended in DMSO or the carrier (DMSO) were added to cultures. Quantification of live cells was performed using trypan blue exclusion dye and counting on a hemacytometer. 10 μ l of cells were diluted 1:2 in trypan blue (Sigma). 10 μ l was loaded onto the hemacytometer and the white live cells excluding trypan blue were counted.

Protein preparation and Immunoblotting

Protein extracts were prepared by cell lysis with 420 mM NaCl Lysis Buffer (20mM Tris pH 7.5, 0.1% BSA, 1mM EDTA, 1% NP-40) supplemented with leupeptin (4 mg/ml), aprotonin (2mg/ml) and phenylmethylsulfonyl fluoride (PMSF) (5mg/ml). Cells were lysed for 30 minutes on ice followed by centrifugation. Protein concentrations were determined by the Bradford

assay. 10-30µg/lane of protein extracts were electrophoresed on a SDS-polyacrylamide (SDS-PAGE) gel and transferred to a PVDF membrane overnight at 4°C. Membranes were blocked for 1 hour in Tris-buffered saline (TBS)-5% milk. Antibodies against cleaved Notch1-val1744 (Cell Signaling Technology) were diluted 1:500 in TBS-5% BSA and incubated with the membrane overnight at 4°C. Blots were washed with TBS 3 x 5 minutes and incubated with HRP-conjugated antibody for 1 hour at RT. For p27, membrane was blocked in 5% milk in TBS supplemented with 0.02% tween-20 and 2% BSA. The anti-p27kip1 antibody was diluted in 10% blocking buffer in TBS supplemented with 0.01% tween.

Histones were prepared by using an acid extraction protocol as detailed on the Upstate Biotechnology web page. Briefly, cells were lysed by using whole-cell lysis buffer containing 0.2 M HCl. After debris was removed by centrifugation, acetone precipitation was performed on the supernatants. Pellets were resuspended in water. Protein concentration was determined by using the Bradford reagent (Bio-Rad) and 30µg was subjected to SDS-PAGE and transferred to PVDF. Membranes were blocked with TBS-3% milk for 1 h and probed with antibody in TBS-3% milk overnight at 4°C, followed by incubation with horseradish peroxidase-conjugated secondary antibody (Jackson Immunoresearch) for 1 h at room temperature. anti-H3, anti-H4, anti-acetyl H3, and anti-acetyl H4 (Upstate Biotechnologies) antibodies were used for Histone western blots.

For other Western blot analyses, anti-Ikaros monoclonal antibody (4E9) (kind gift of Katia Georgopoulos, Massachusetts General Hospital and Harvard Medical School) was used. For these blots, PVDF was blocked in 5% milk in TBS for 1 hour. Antibodies were diluted 1:1000 and incubated with the membrane for 1 hour. Membranes were washed in TBS 3 times

for 10 minutes and secondary antibody was added to blots at a dilute of 1:5,000 in 20mL of 5% Milk in TBS for 1 hour. Washes were repeated. Enhanced chemiluminescence reagent was utilized to visualize proteins. Densitometry was performed by using a Multi-Image light cabinet (Alpha Innotech Corporation).

Retroviral Constructs

Sequences corresponding to Ikaros isoform Ik-1 were PCR amplified from cDNA generated from mouse T cells. Sequences corresponding to Ik-7 were PCR amplified from DNA obtained from an Ik-7 transgenic mouse line. In both cases sequences corresponding to the flag epitope were introduced at the N-terminus. Flag-Ik-1 and Flag-Ik-7 cDNA sequences were subcloned into the murine stem cell virus internal ribosome entry site green fluorescing protein (MSCV IRES GFP) construct and MSCV IRES H-2K^k vectors (Clontech). Sequencing was then performed through the Sequencing core facility at the University of Chicago to ensure fidelity of PCR amplification. CDNAs encoding the p27kip1 vector were obtained from the American Tissue Culture Center. They were cloned directly into the MSCV IRES H-2Kk retroviral vector. MSCV IRES Hes1 GFP was a gift of Dr. Warren Pear (University of Pennsylvania, Philadelphia, PA).

Ikaros mutants were generated by site directed PCR mutagenesis (92). 5' and 3' end primers used to insert restriction enzyme sites for cloning were (5' to 3'): 5' extension (BglII), GCC GAC CGT CAG ATC TAT GGA CTA CAA GGA CGA CGA TGA CAA G; 3'extension (XhoI), GCT GTA GGA ATT CGC TGT AGC TCG AGT TAG CTC AGG TGG TAA CGA TGC TCC. Mutation introducing primers: F2 DBD forward, GCC TCC TTT ACC CGG AAA

GGC AAC CTCC; F2 DBD reverse, GGA GGT TGC CTT TCC GGG TAA AGG AGG C; F3 DBD forward, TGC CTG CCG CCA GAG GGA CGC CCT; F3 DBD reverse, AGG GCG TCC CTC TGG CGG CAG GCA; F2M forward, CCT TTC CAG GGC AAC CAG GGT GGG GCC T; F2M REVERSE AGG CCC CAC CCT GGT TGC CCT GGA AAG G; F3M forward, GAA GCC CTT CAA AGG CCA TCT TGG CAA CTA TGC CTG; F3M reverse, CAG GCA TAG TTG CCA AGA TGG CCT TTG AAG GGC TTC. Following BglIII-XhoI restriction enzyme digest of PCR products, mutant Ik-1 sequences were subcloned into MSCV IRES H-2Kk.

Retroviral Transduction

Retroviral plasmid constructs were transfected into Phoenix ecotropic packaging cells using Lipofectamine reagent (Invitrogen). Viral supernatants were harvested at 48 and 72 hours postinfection, passed through a 0.22µm filter and stored at -80°C. JE131 cells were infected using 500ul-1ml of supernatant per 2×10^6 cells supplemented with 8 µg/ml of polybrene in a 24 well tissue culture plate. Plates were centrifuged at 500 x g for 2 hours at 32°C. Supernatants were removed and cells were cultured with RPMI complete medium.

Cell Sorting

Successfully transduced cells were sorted by either high speed MoFlo flow cytometer or with the MiniMacs system (Miltenyi) using the H-2K^k expression marker. For H-2K^k sorting, JE131 cells were trypanized to disperse clumped cells and prevent further clumping. This was followed by a centrifugation gradient step through Histopaque-1083 to remove dead cells. Cells were incubated with the H-2K^k antibodies coupled to magnetic beads and run over magnetic

column that retains labeled positive cells. H-2K^k expression was analyzed using either anti-bead FITC conjugated antibody or by anti H-2K^k FITC antibody. Purity was assessed using the MACSelect control fluorescein isothiocyanate (FITC) antibody or FITC conjugated H-2K^k if tested 24 hours post-infection. Purity was consistently > 90%.

Antibodies

For flow cytometric analyses, the following antibodies were used: anti-CD4 (GK1.5, eBiosciences), anti-CD8 (53-6.7, eBiosciences), anti-TCR_β (H57-597), anti-CD5 (53-7.3), anti-CD69 (H1.2F3), MACSelect control FITC antibody (Miltenyi Biotech), and anti-H-2K^k (H100-27.R55, Miltenyi Biotech). Antibodies were allophycocyanin (APC), FITC, or phycoerythrin (PE) conjugates. For staining, cells were plated in microwell staining plates at 5×10^5 to 1×10^6 cells per well. Fluorochrome conjugated antibodies were added to cells and incubated on ice for 15 minutes. Stained cells were analyzed by flow cytometry on a FACScalibur (BD Biosciences) flow cytometer using CellQuest Pro software.

Cell staining and flow cytometry

Cells were plated in microwell staining plates at a density of 5×10^5 to 1×10^6 cells/well. Cells were blocked in rat serum for 10 minutes at 4° prior to staining. Fluorochrome-conjugated antibodies were added to cells and incubated on ice for 15 to 20 min. Cells were then washed in PBS/2% FCS/1mM EDTA and fixed in 75μl of 2% paraformaldehyde, followed by the addition of an equal volume of phosphate-buffered saline-1% BSA. Fixed cells were analyzed 12 to 72 h

later on a FACSCalibur (BD Biosciences) flow cytometer. Analyses were performed on Cellquest Pro or FlowJo software.

RT-PCR

mRNA was prepared with Trizol reagent (Invitrogen) or using the total RNA isolation kit (Promega) from H-2K^k positive retrovirally transduced JE131 cells sorted 24 hours postinfection or JE131 cells treated with DAPT for 36 hours. RNA was resuspended or eluted in 50ul RNase free water. RNA prepared using trizol was incubated with RNaseOUT (320U/mL), RNase-free DNase (100U/mL), and MgCl₂ (1.5mM, Invitrogen) for 30 minutes at 37°C to remove genomic DNA contamination. RNA was cleaned using Rneasy Mini Kit (Qiagen). cDNA was generated using a Superscript II kit (Invitrogen). For semi-quantitative PCR, three-fold dilutions were performed on cDNA and HPRT concentrations were normalized. Primers used for conventional PCR are as follows: p27kip1, CCC GCC CGA GGA GGA AGA TGT CAA AC and CCC TTT TGT TTT GCG AAG AAG AAT CT; p21, CCG TGG ACA GTG AGC AGT TG and TGG GCA CTT CAG GGT TTT CT; cyclin D2, AGA CCT TCA TCG CTC TGT GC and TAG CAG ATG ACG AAC ACG CC; Hes1 forward, ATG CCA GCT GAT ATA ATG GAG; Hes1 reverse, ACG CTC GGG TCT GTG CTG AGC; hypoxanthine phosphoribosyltransferase (HPRT), GTT GGA TAC AGG CCA GAC TTT GTT G and GAG GGT AGG CTG GCC TAT AGG CT.

Quantitative real-time RT-PCR (qRT-PCR) was performed using a Bio Rad iQ5 Real Time PCR machine and either iQ SYBR Green Supermix (Bio-Rad) or TaqMan probes. For the probes, the 5' and 3' ends of the probes were labeled with fluorescent dyes FAM (6-

carboxyfluorescein) and TAMRA (6-carboxy-tetramethyl-rhodamine) (TaqMan technology). Primer pairs were designed to flank their respective TaqMan probes. Primer and probe sequences used (5' to 3'): Hes1 forward, GCC AAT TTG CCT TTC TCA TCC C; Hes1 reverse, CCT AAC GCA GTG TCA CCT TCC; Hes1 probe, CAGCAACAGTGGGACCTCGGTGGG; Deltex1 forward, GGC CAA AAC AAC CTC AGT CG; Deltex1 reverse, GAA GAA CTT GAA TGG CAC TGG C; Deltex probe, CAC AGA GGT CCA CCA GCG TCA GCG. HPRT. Primers used for SYBR green qPCR: Hes1 forward, GCC AAT TTG CCT TTC TCA TCC C; Hes1 reverse, CCT AAC GCA GTG TCA CCT TCC; Deltex1 forward, GGC CAA AAC AAC CTC AGT CG; Deltex1 reverse, GAA GAA CTT GAA TGG CAC TGG C; Hprt forward, TGG GCT TAC CTG ACT GCT TTC; Hprt reverse, CCT GGT TCA TCA TCG CTA ATC AC. Analyses of qRT-PCR were performed using the Pfaffl method. Primers were designed using Beacon Design software and synthesized by IDT DNA Technologies.

Cell cycle analysis and Pyronin Y staining

For cell cycle analysis, 10^6 successfully transduced cells were pelleted, washed in phosphate-buffered saline, and fixed in cold 70% ethanol overnight. Cells were stained with propidium iodide, followed by analysis on a FACSCalibur (BD Biosciences, Mountainview, Calif.) flow cytometer. The ModFit Cell Cycle analysis program was used to determine the percentages of cells at each stage of the cell cycle. Pyronin Y staining was performed as previously described (43). Briefly, sorted GFP+ and GFP- cells were fixed in 70% ethanol. Cells were incubated with 2 μ g of Hoechst stain per ml and 4 μ g of Pyronin Y per ml for 20 min prior to running on the flow cytometer (Beckman Coulter Elite ESP).

Chromatin Immunoprecipitation

Chromatin immunoprecipitation (ChIP) was performed using chromatin prepared from H-2K^k positive JE131 cells infected with MSCV IRES H-2K^k or MSCV IRES Ik-1 H-2K^k retroviruses at 24 hours postinfection using the ChIP Assay Kit (Upstate). Briefly, 10⁶ cells were used per sample. Proteins bound to DNA were cross-linked by treating cells with 1% formaldehyde for 10 minutes at RT. Cells were washed, lysed, and sonicated (Fisher Scientific Sonic Dismembrator Model 100) to shear DNA. Samples were precleared with Protein G or Protein A Agarose/Salmon Sperm beads (Upstate). Protein-DNA complexes were immunoprecipitated using antibodies against Ikaros, RBP-J (Santa Cruz and Chemicon), anti-acetylated histone H3 (Upstate) or a control IgG (Santa Cruz). Complexes were collected with Protein G or Protein A Agarose/Salmon Sperm beads and washed. Protein-DNA complexes were eluted off the beads and crosslinks were reversed by heating at 65 °C overnight. DNA was recovered by phenol:chloroform extraction and precipitated by ethanol. Quantitative real-time PCR (qPCR) analyses were performed on immunoprecipitated DNA and normalized to total chromatin input using the Pfaffl method. Primers were used with iQ SYBR Green Supermix (Bio-Rad) and were as follows (5' to 3'): Hes1 forward, CTG TGG GAA AGA AAG TTT GGG AAG; Hes1 reverse, GCT CCA GAT CCT GTG TGA TCC; Upstream 1.2kb F, CTC CCT TGT CCG CCG TCT ATC C; Upstream 1.2kb R, CGC TCG TTC CTC CGC CAC TCT C; Upstream 7kb F, GAG AGG CAA CCA CGG ACT TG; Upstream 7kb R, ACA GGC TCC AGG CAC CAC; Downstream 1.8kb F, GCG TGC GTC CCC TCT CTG; Downstream 1.8kb R, GCT GAA TGC CTC TCA CAA CCG; Downstream 2.5kb F, GCG GCT CCC AAC TCA CTC C;

Downstream 2.5kb R, ACA GAC AAA TGA AGG TCC CAA TGC; Deltex 1 forward, CTA TGT ACC TAT GTC CTC AGA TGC; Deltex1 reverse, CTT CTC GGG CTT CCA ACC TC.

Chromatin Immunoprecipitation Western Blot

For ChIP-Western, chromatin immunoprecipitation was performed with anti-Ikaros monoclonal antibodies or control IgG. Chromatin utilized was derived from 5×10^6 magnetically sorted H-2Kk positive JE131 cells infected with MSCV IRES H-2Kk or MSCV IRES Ik-1 H-2Kk retroviruses. Immunoprecipitated complexes were eluted from Protein G agarose/salmon sperm DNA beads by incubation in Laemmli buffer at 95° C for 10 minutes and subjected to Western blot analyses using antibodies against RBP-J (Chemicon) or Ikaros.

Chapter III.

Ikaros induces quiescence and T cell differentiation in JE131 cells

Introduction

Targets of deregulation in cancer cells are often nuclear factors that have the ability to change gene expression. A well-characterized mutation often found in leukemia, cancer of cells in the hematopoietic lineage, occurs in the RUNX1/AML1 gene. RUNX1/AML1 mutations are often translocations of different genes that disrupt the normal function of the transcription factor and/or the other component of the translocation. These mutations result in inactivation of RUNX1/AML1, which is required for regulation of transcription, both through activation and repression (93-95). In addition to AML, evidence suggests that other transcription factors are deregulated, which can result in leukemogenesis (96).

Ikaros, like AML, is a regulated nuclear factor that contains a DNA-binding domain (24, 25). All reported cases of childhood acute lymphocytic leukemia (ALL) have defects in Ikaros expression that decrease Ikaros activity and defects in Ikaros have been found in many other types of leukemia (97-99). Ikaros is a member of the Ikaros family of proteins, all of which contain zinc-finger protein-protein interaction domains (24, 25). There are six isoforms of Ikaros, which differ in the number of exons by alternative splicing (25). Isoforms Ik-1, Ik-2 and Ik-3 contain a DNA binding domain, while Ik-4 though Ik-6 do not (26). Ik-4, 5, 6 are often overexpressed in leukemia and are believed to have a dominant negative effect on DNA binding

competent isoforms through oligomerization (29, 34, 100). The absence of the DNA binding domain reduces Ikaros' ability to regulate transcription, because in the absence of a DNA binding domain, Ikaros can no longer bind to DNA and recruit other components of the chromatin remodeling complexes to targeted loci (26). These data support the hypothesis that loss of Ikaros is a key factor in the leukemic process.

In addition, genetically altered mice that are homozygous null for Ikaros develop leukemia with 100% penetrance within six weeks of birth and Ikaros is highly conserved between mice and humans (33, 34). The early onset and totality at which the mice develop leukemia when deficient for Ikaros further suggests a role for loss of Ikaros in development of leukemia.

To define Ikaros as a tumor suppressor, it must fulfill two requirements. Absence of Ikaros must result in uncontrolled proliferation (33) and reintroduction of Ikaros to Ikaros null cells must result in growth arrest. This chapter provides evidence that Ikaros fulfills these requirements.

Results

Reintroduction of Ikaros into the Ikaros null T cell line

An Ikaros null cell line was generated from thymocytes obtained from an Ikaros null mouse with spontaneously arising leukemia. The thymocytes were removed from the mouse, plated in cell culture growth medium, and allowed to proliferate. We named this cell line the JE131 Ikaros null T cell line. These cell surface phenotype is Thy1⁺, CD4⁻, CD8⁻, TCR⁻, CD44⁻, CD25⁺,

which resembles the surface marker expression in thymocytes at the DN3 stage of T cell development.

In order to examine the role of Ikaros in the Ikaros null JE131 cell line, a retroviral transduction system was utilized to introduce Ikaros to the cells. Two different retroviral vectors, MSCV IRES GFP and MSCV IRES H2K (**Figure 1**) were used. The MSCV long terminal repeat promoter and enhancer sequences give rise to high levels of expression of the genes encoded by the vector in T cells (101). The internal ribosomal entry site (IRES), allows for transcription of either the green fluorescent protein (GFP) or a truncated MHC class I protein, H-2K^k (H2K). Both GFP and H2K serve as markers for infection and allow for sorting of cells based on GFP or H2K expression. GFP sorting was performed on a high speed sorting flow cytometer (R.H. Lurie Comprehensive Cancer Center). H2K expressing cells were sorted using anti-H2K antibodies conjugated to magnetic beads (Miltyni), as H2K is expressed on the cell surface. Both vectors were used interchangeably with similar results.

cDNAs encoding two Ikaros isoforms, Ik-1 and Ik-7 (**Figure 1**), were subcloned into the MSCV retroviral vectors to generate MSCV Ik-1 IRES GFP or MSCV Ik-1 H-2K (Ik-1) and MSCV Ik-7 IRES GFP or MSCV Ik-7 H-2K (Ik-7). Ik-1 was chosen as it is the full-length isoform of Ikaros containing all exons and is most highly expressed in T cells. Ik-7, a laboratory engineered, non-DNA binding form of Ikaros that lacks exons 2 and 3 which encode 3 of the 4 N-terminal zinc fingers, was used as a control (26). Without the necessary N-terminal zinc fingers, Ik-7 cannot bind DNA, therefore, any differences observed between the activities of Ik-1 and Ik-7 implicate the DNA binding activity of Ikaros as the mediator of changes detected upon

reintroduction (26). All experiments performed included use of the MSCV IRES H2K or GFP (MSCV) as a negative control.

To generate virus for infection of T cells, the Phoenix packaging cell line was used (101) (**Figure 4**). This derivative line of 293T cells contains episomal *gag*, *pol* and *env* genes and are easily transfected using a lipid transfection system (102). The MSCV constructs were transfected into the Phoenix cells using Lipofectamine. Supernatants were harvested from the cells and used to infect JE131 cells, the Ikaros null T cell line. Twenty-four hours post-infection, successfully transduced cells were sorted by cell surface expression of H2K or GFP expression. Protein extracts were prepared from sorted cells and a Western blot for Ikaros expression was performed. Expression of Ikaros in transduced cells was compared to Ikaros expression in wild-type thymocytes (**Figure 5**). Importantly, levels of Ikaros approximate those observed in the wild-type thymocytes.

Cell counts were also performed on sorted JE131 cells expressing Ikaros. These counts were carried out using a haemocytometer at 24-hour intervals for eight days. Trypan Blue was used to stain the dead cells. JE131 cells not expressing either Ikaros isoform have a similar growth rate to that of JE131 cells transduced with Ik-7. In cells transduced with Ik-1, however, the growth rate is significantly decreased, indicating that Ik-1 transduced JE13 cells have a reduced growth potential compared to cells transduced with the control viruses (**Figure 6**). However, by day 8, the growth rate of JE131 cells expressing Ikaros increased. Therefore, expression levels of H2K were examined to determine if loss of Ikaros expression could account for the increased growth rate of these JE131 cells. To this end, expression of H2k was analyzed over time in JE131 cells transduced with retroviruses containing one of the following constructs,

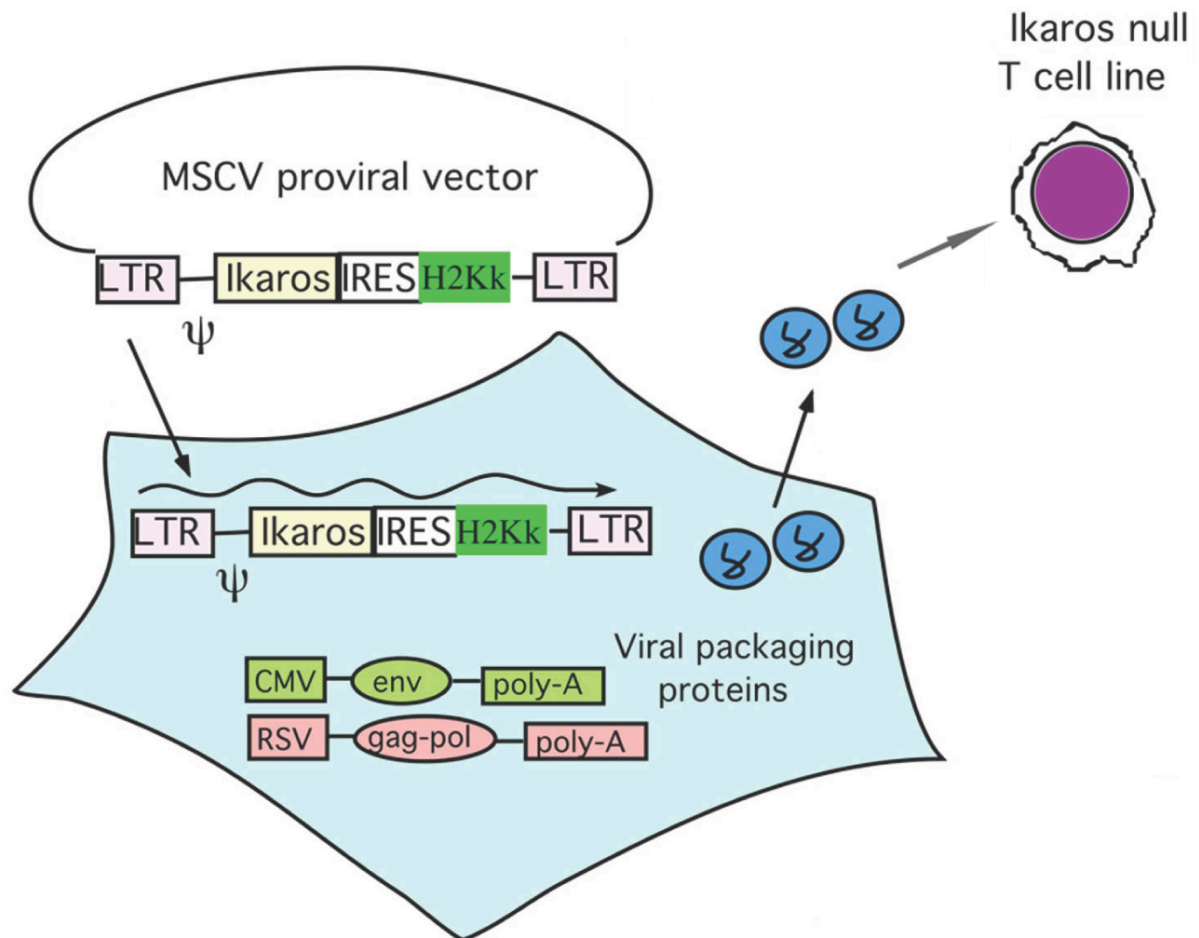


Figure 4. Phoenix cell retroviral transduction system. MSCV proviral vector (MSCV Ikaros H-2Kk is shown, MSCV Ikaros GFP was used interchangeably) was introduced by lipofection into Phoenix cells. Supernatants produced by Phoenix cells were harvested and used to infect JE131 cells.

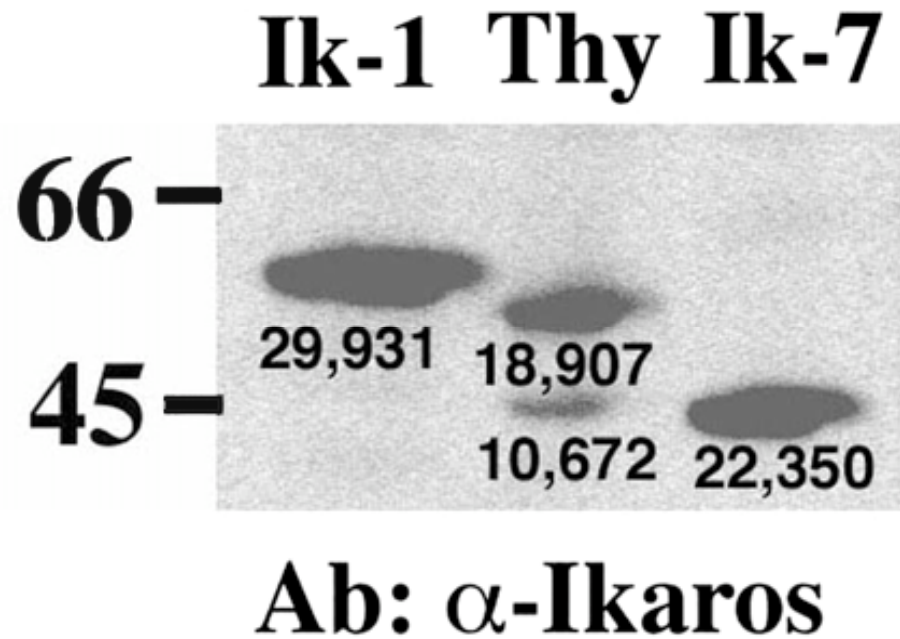


Figure 5. Retroviral expression levels of Ik-1 are comparable to expression levels of DNA-binding Ikaros isoforms in wild-type thymocytes. Whole cell extracts of wild-type thymocytes (Thy) and purified JE131 cells successfully transduced with the MSCV Ik-1 H2K (Ik-1) or the MSCV Ik-7 H2K (Ik-7) retroviruses were prepared. 10 µg of protein was subjected to SDS/PAGE, and Western blotting was performed with an anti-Ikaros monoclonal antibody. The two Ikaros bands visible in the wild-type thymus (Thy) correspond to the predominantly expressed Ikaros isoforms, Ik-1 (top band), and Ik-2 and Ik-3, which co-migrate (bottom band). The Ik-1 band in the retrovirally transduced cells is of slightly larger molecular weight due to the flag epitope tag. Densitometry readings are shown under each band. Blot performed by Erin Griffiths.

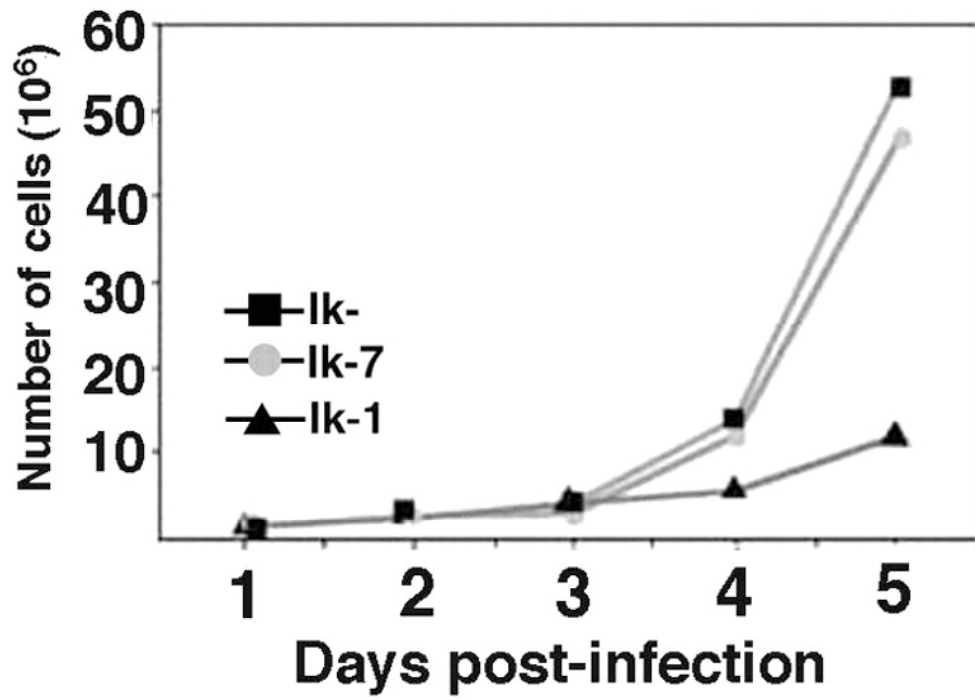


Figure 6. Re-introduction of Ikaros into the JE131 cells has a profound effect on their growth properties. JE131 cells were infected with the MSCV H2K (Ik-), MSCV Ik-7 H2K (Ik-7) or MSCV Ik-1 H2K (Ik-1) retroviruses. Successfully transduced cells were purified and plated at 1×10^6 cells/well in a 24-well plate. Counts of viable cells were performed every 24 hours.

Ik- (vector control), Ik-7 or Ik-1. FACS analysis of H2K expression in these cells was performed using an anti-H2K FITC antibody at 24-hour intervals. Compared to Ik- and Ik-7, a decrease in the percentage of Ik-1 infected JE131 cells expressing H2K was observed over time. This illustrates that Ik-1 transduced JE131 cells shut off expression of the H2K marker over time (**Figure 7a**).

Ikaros expression in these cells was also analyzed to compare loss of H2K with loss of Ikaros expression. Whole cell extracts from JE131 cells expressing no Ikaros (Ik-), Ik-7 or Ik-1 were prepared and subjected to Western blotting. Consistent with the decreased expression of H2K, the small percentage of JE131 cells still expressing H2K on day 8 also have dramatically decreased levels of Ik-1 expression. This is compared to Ik-7 transduced cells at day 8 which retain high levels of Ik-7 expression (**FIGURE 7b**). These data suggest that in order for Ik-1 transduced cells to grow in culture they must significantly down-regulate or turn off Ik-1 expression.

Upon FACS analysis of JE131 cells infected with Ik-, Ik-7 and Ik-1 containing retroviruses, a “small cell” population was observed in JE131 cells expressing Ik-1 (**Figure 8, R2**). This unique population was found to have low forward and side scatter and began to appear at 48 hours post infection. The population size peaks between 72 to 96 hours post infection, then steadily decreases. The absence of a “small cell” population in JE131 cells expressing Ik-7 suggests that the DNA binding ability of Ikaros is essential for the formation of this population.

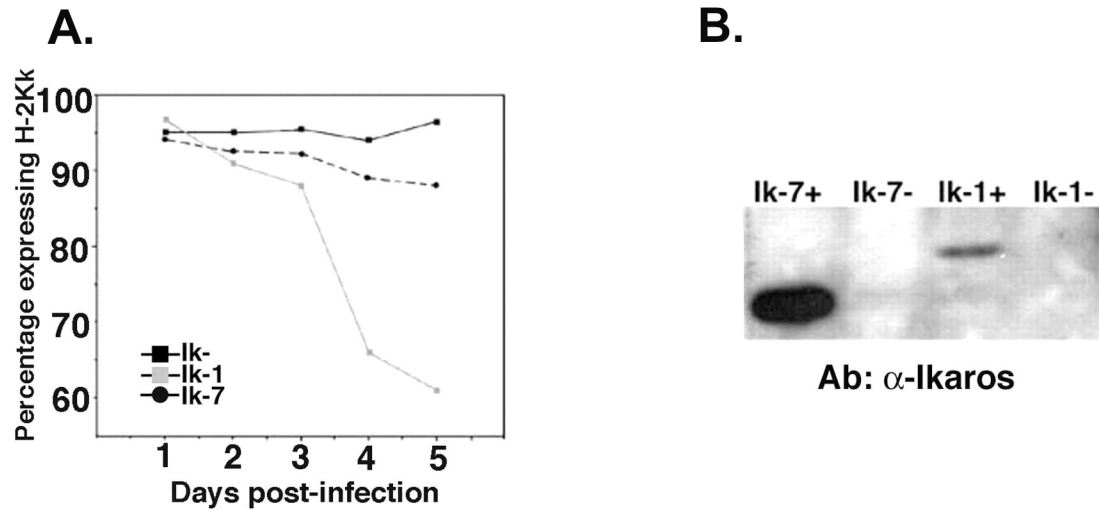


Figure 7. Reintroduction of Ikaros to JE131 cells results in loss of H-2Kk and Ikaros expression after 5 days in culture. JE131 cells were infected with the MSCV H2K (Ik-), MSCV Ik-7 H2K (Ik-7) or the MSCV Ik-1 H2K (Ik-1) retroviruses. Successfully transduced cells were purified and plated at 1×10^6 cells/well in a 24-well plate. **(A)** H2K (H-2Kk) expression as monitored every 24 hours in the purified cell populations by flow cytometry. **(B)** After 8 days in culture, cells were resorted for H-2K expression and whole cell protein extracts were prepared from H2K+ and H2K- fractions. 10 μ g of protein were loaded onto an SDS/PAGE gel and Western blotting was performed with an anti-Ikaros monoclonal antibody.

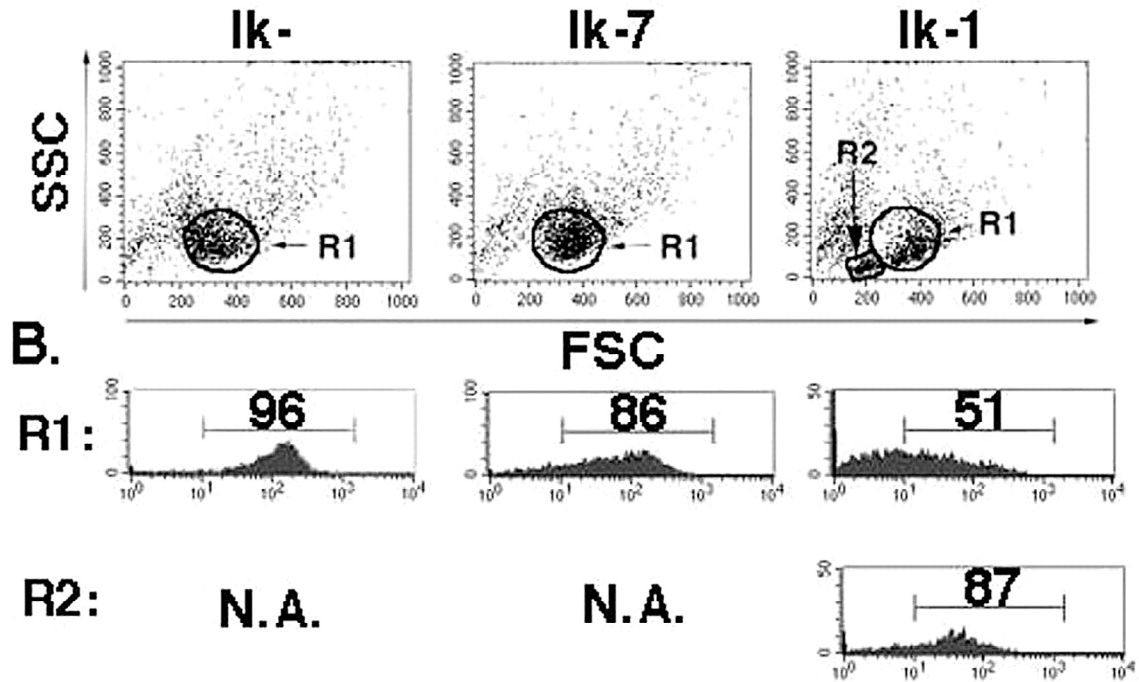


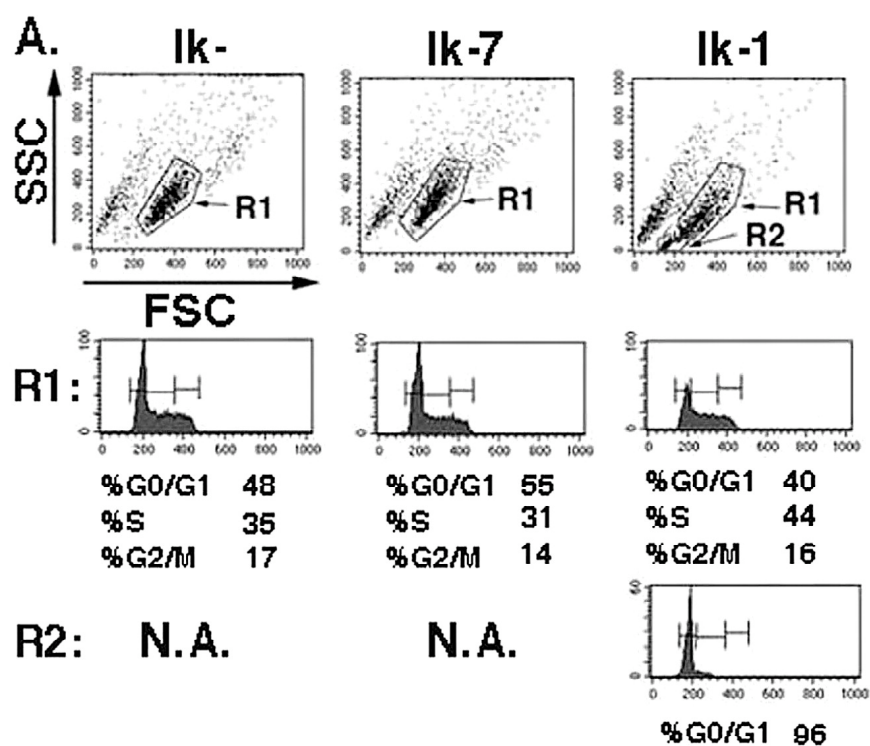
Figure 8. Appearance of a “small cell” population in Ik-1 expressing JE131 cells. Forty-eight hours after infection, JE131 cells infected with the MSCV H2K (Ik-), the MSCV Ik-7 H2K (Ik-7) or the MSCV Ik-1 H2K (Ik-1) retrovirus were stained with fluorochrome conjugated anti-H2K, and flow cytometric analysis was performed. (A) A unique population of cells with low forward and side scatter (R2) was observed in the Ik-1 transduced culture. (B) This effect is confined to successfully transduced cells, since the “small cell” population is almost uniformly H2K+, and, therefore, Ik-1+. The larger cell population (R1) is already beginning to lose H2K, and therefore, Ik-1 expression.

JE131 cells transduced with Ik-1 arrest in G0/G1

The reduced growth potential observed in Ik-1 transduced JE131 cells suggests that these cells may be undergoing cell cycle arrest. To examine this possibility, JE131 cells expressing Ik-7, Ik-1 or not expressing Ikaros (Ik-) were fixed with 95% ethanol at 24 hour intervals and stained with propidium iodide for analysis by flow cytometry. Propidium iodide is a dye that intercalates into DNA, allowing for measurement of DNA content, which correlates with cell cycle status. Cell cycle analyses of JE131 cells expressing Ik-1 showed the dramatic effects of Ikaros reintroduction in these cells as early as 24 hours post infection (**Figure 9a**). Cells transduced with Ik-1 accumulate in the G0/G1 stage of cell cycle, while JE131 cells not expressing Ikaros or transduced with Ik-7 display typical cell cycle profiles of proliferating cells. To differentiate between G0 and G1, JE131 cells were stained with Pyronin Y, a cytoplasmic RNA dye. Cells in G1 stain positively with Pyronin Y, while G0 cells do not. 89% of Ik-1 infected JE131 cells fail to stain strongly with Pyronin Y, compared to 0.2% in the control (**Figure 9b**). This suggests the transcriptional shutdown in the Ik-1 transduced cells, indicating that JE131 cells expressing Ik-1 undergo a cell cycle exit at the G0 phase of the cell cycle.

The cell cycle arrest and the appearance of a “small cell” population could suggest the Ik-1 expressing JE131 cells were undergoing apoptosis. In non-apoptotic cells, phosphatidylserine (PS) faces the cytosolic side of the cell membrane. However, a marker of apoptosis is the loss of phospholipid symmetry in the outer cell membrane and involves the appearance of PS on the surface of cells. Annexin V is a protein that binds to negatively charged phospholipids, such as PS (103). When conjugated to a fluorescent marker, it can be used to detect the appearance of PS on the surface of cells by FACS analysis, thereby indicating cells

Figure 9. “Small cell” population of Ik-1 expressing cells are arrested at G0/G1. (A) Three days after infection of the JE131 cells with MSCV H2K (Ik-), MSCV Ik-7 H2K (Ik-7) or MSCV Ik-1 H2K (Ik-1) retroviruses, DNA content was analyzed by propidium iodide staining as a measure of cell cycle status. Cells which fall into the R1 gate show similar cell cycle profiles in all three transduced cultures. However, the unique small cell population (“R2”) observed in the Ik-1 transduced culture is blocked at the G0/G1 phase of the cell cycle. (B) At day six post-infection, successfully transduced cells were sorted from the cultures and Pyronin Y staining was performed to measure cytoplasmic RNA content. Pyronin Y negative cells are in G0 whereas Pyronin Y positive cells are in G1, S or G2/M. The majority of Ik-1 transduced cells fell into the “small cell” population and failed to stain with Pyronin Y.



B.

| Population tested | % "small cells" | Pyronin Y negative | Pyronin Y positive |
|-------------------|-----------------|--------------------|--------------------|
| Ik- | 4.3 | 0.2% | 99.3% |
| Ik-1 | 80 | 89% | 9% |
| Ik-7 | 4.1 | 1.3% | 98.6% |

undergoing apoptosis. JE131 cells transduced with Ik-, Ik-7 or Ik-1 were stained with annexin V-PE and analyzed by FACS. All populations of JE131 cells stained negatively for annexin, indicating that there is no increase in the amount of apoptosis in JE131 cells expressing Ik-1 (**Figure 10**).

Cell Cycle Regulator as a Target for Ikaros

The reduced growth kinetics and cell cycle arrest observed in the JE131 cells expressing Ikaros suggest that Ikaros could be functioning to alter expression of one or more cell cycle regulators. Given that the JE131 cells expressing Ikaros are at the G0/G1 phase of the cell cycle, we focused our analyses on cell cycle inhibitors that function at that stage. Two families of cell cycle inhibitors, Kip/Cip and INK4, are possible targets for the changes in growth observed upon reintroduction of Ikaros to JE131 cells. The Kip/Cip family consists for p27kip1 (p27), p21WAK/Cip-1 (p21) and p57kip2. This family of inhibitors negatively regulates cyclin dependent kinases (cdks) and their cyclin counterparts (104, 105). The Ink4 family consists of p15INK4B (p15), p16INK4a (p16), p18INK4c and p19INK4d. These proteins inhibit cdk4 and 6 (106).

Using cDNA and whole cell extracts from JE131 cells not expressing Ikaros or expressing Ik-1, expression levels of these genes were examined. Cells were infected with Ik- and Ik-1 retroviruses and sorted for H2K expression after 24 hours. After sorting, mRNA was prepared from the cells and reverse transcribed using random hexamers (Qiagen) to generate cDNA. The cDNA was then subjected to PCR with primers for different cell cycle genes to test for changes in expression of cell cycle regulators in JE131 cells expressing Ikaros. Whole

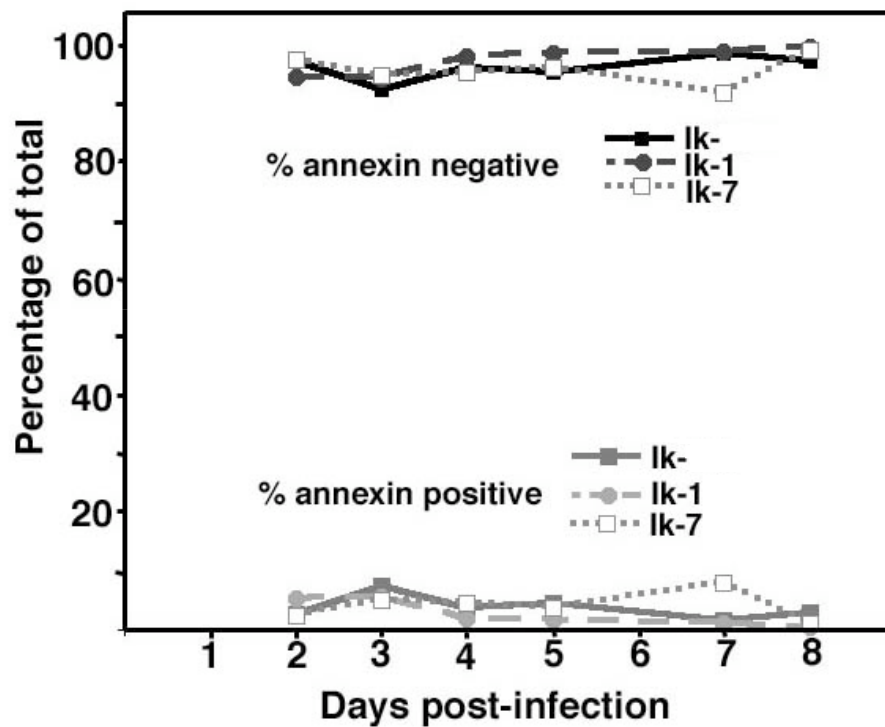


Figure 10. Percent of cells undergoing apoptosis is equal among transduced JE131 cells. JE131 cells were infected with MSCV H2K (Ik-), MSCV Ik-1 H2K (Ik-1) or MSCV Ik-7 H2K (Ik-7) retroviruses and sorted for H2K expression. Cells were stained with annexin V at 24 hour intervals for 8 days.

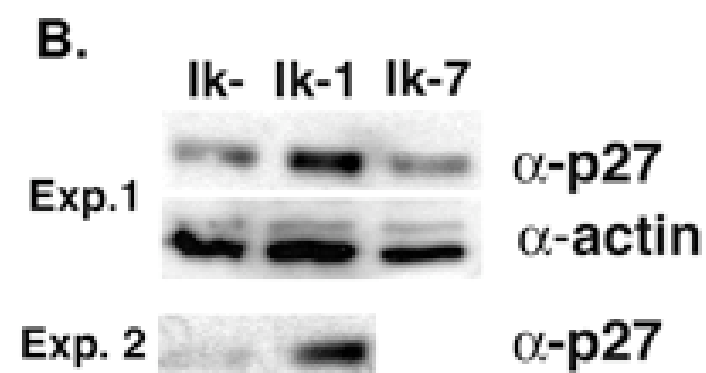
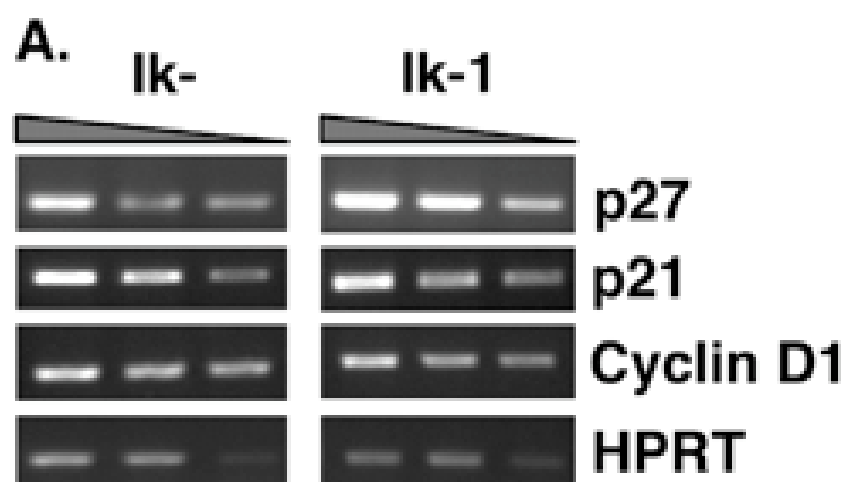
cell extracts were also prepared from sorted cells to analyze protein expression of cell cycle regulators.

By RT-PCR, we observed no difference in expression levels of *cyclin D1* or *p21* between JE131 cells transduced with Ik-1 and those transduced with the control virus that express no Ikaros (**Figure 11**). No difference in expression of p15 and p16 was detected by Western blot (data not shown). However, an increase in expression of *p27* mRNA was observed between JE131 cells transduced with vector and Ikaros retroviruses, suggesting a role for Ikaros in regulation of *p27* expression (**Figure 11a**). Protein extracts from JE131 cells expressing Ikaros also showed elevated levels of p27, indicating that increased levels of *p27* mRNA led to increased protein expression of p27 (**Figure 11b**).

To further examine the growth suppressive role of p27 in JE131 cells, cDNA encoding *p27* (ATCC) was subcloned into the MSCV IRES GFP vector. This was used to compare growth in JE131 cells transduced with Ikaros to those with an overexpression of p27. If upregulation of *p27* contributed to growth arrest in Ik-1 transduced cells, it was expected that expression of p27 in the Ikaros null JE131 cells would mimic the growth arrest seen in the cells where Ikaros was reintroduced. JE131 cells were infected with retroviruses containing p27, Ik-1, or the control vector (Ik-), sorted and plated at equal numbers. Cells were counted at 24-hour intervals. JE131 cells transduced with p27 display similar growth kinetics as those observed in JE131 cells expressing Ikaros (**Figure 12**). Upon cell cycle analysis of the JE131 cells expressing p27, it was observed that expression of p27 also results in an accumulation in G0/G1, similar to that observed in JE131 cells expressing Ikaros. This was not unexpected, as

Figure 11. Ik-1 transduced JE131 cells display an increase in p27kip1 expression JE131 cells with and without Ik-1 activity were analyzed for RNA and protein expression of p27kip1

(A) Twenty four hours after infection with the MSCV GFP (Ik-) or MSCV Ik-1 GFP (Ik-1) retrovirus, successfully transduced JE131 cells were purified, and cDNA prepared. RT-PCR was performed using a range of cDNA amounts. Shown here are the results of two-fold dilutions (from 1:256 to 1:1024 for each sample). **(B)** Twenty four hours after infection with Ik-1, MSCV Ik-7 GFP (Ik-7) or Ik- retroviruses, successfully transduced JE131 cells were purified, and protein extracts were prepared. 10 μ g of protein was subjected to SDS/PAGE. Blots were probed with antibodies against p27kip1 or actin (as a loading control). Results from two representative experiments are shown.



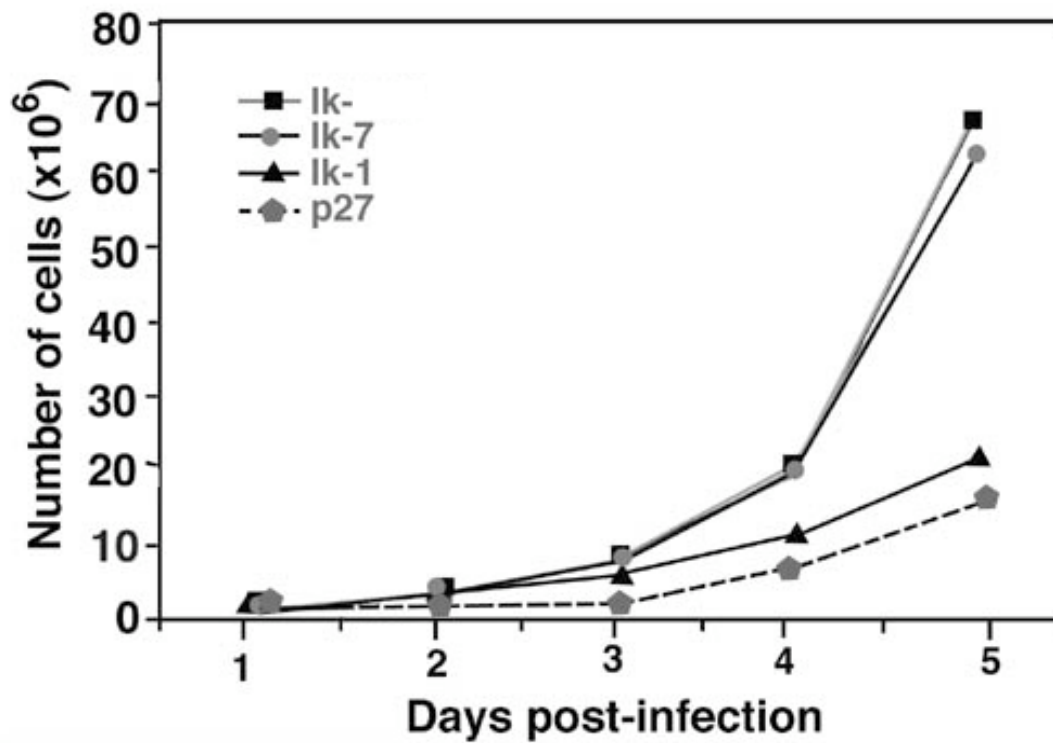


Figure 12. Growth of JE131 cells can be slowed by retroviral transduction of p27kip1.

JE131 cells were infected with the MSCV H2K (Ik-), MSCV Ik-7 H2K (Ik-7), MSCV Ik-1 H2K (Ik-1) or MSCV p27kip1 H2K (p27) retroviruses. Successfully transduced cells were purified and plated at 1×10^6 cells/well in a 24-well plate. Counts of viable cells were performed every 24 hours.

p27 is a cell cycle regulator that acts at the G0/G1 phase of the cell cycle. However, it is important to note the parallel growth curves and similar percentages of cells in G0/G1 between JE131 cells expressing p27 and those expressing Ikaros. However, the growth arrest observed in JE131 cells expressing p27 occurred more rapidly than in Ikaros expressing JE131 cells. This could be the result of two steps required in JE131 cells expressing Ikaros; transcription and translation of Ikaros, then transcription and translation of p27, whereas JE131 cells expressing p27 need only transcription and translation of p27.

Next, we wanted to determine if Ikaros plays a direct role in regulation of *p27*. To address this possibility, we utilized two techniques, luciferase assays and chromatin immunoprecipitation. However, neither of these techniques suggested that Ikaros directly regulates *p27* expression (data not shown). Therefore, we hypothesized that Ikaros must regulate another unknown factor that contributes to the increase in *p27* expression.

JE131 cells expressing Ikaros undergo a T cell differentiation program

Cell cycle arrest can serve as a marker for differentiation and expression of p27 has been shown to correlate with differentiation (55). Thus, we hypothesized that the appearance of a “small cell” population and the cell cycle arrest observed in JE131 cells expressing Ikaros may also indicate that these cells were undergoing differentiation (**Figure 13a**). To examine this possibility, JE131 cells were transduced with Ik-7 or Ik-1 or no Ikaros and stained with fluorochrome-conjugated antibodies for T cell differentiation markers 72-96 hours post-infection. The markers selected were CD4, CD8, CD25, CD5, CD69 and TCR. These specific markers were chosen as their expression changes upon transition from the DN to DP stage of T

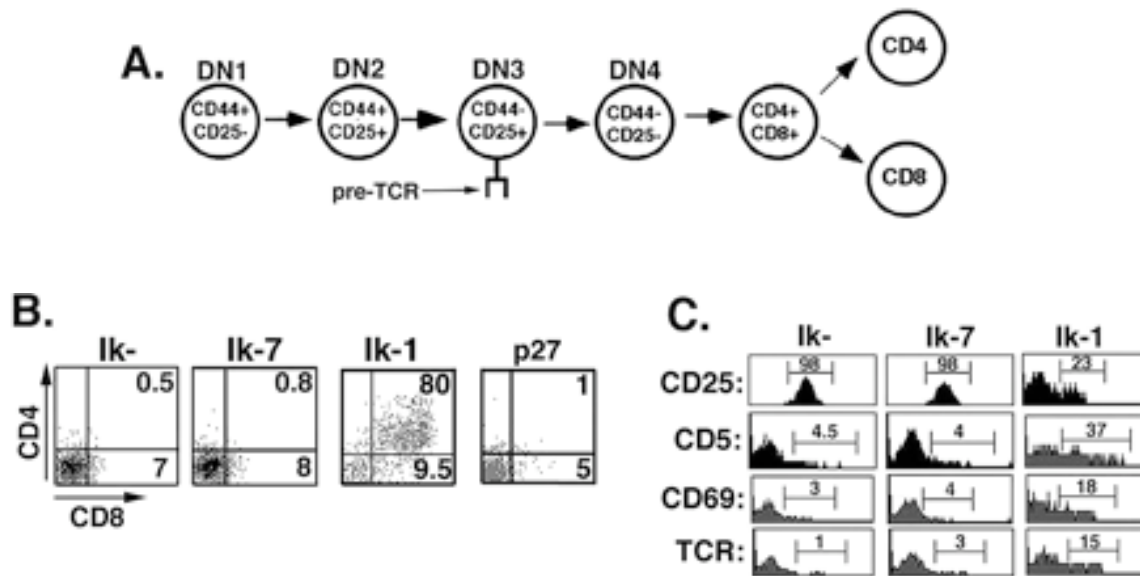


Figure 13. Reintroduction of Ik-1 into JE131 cells induces a T cell differentiation program.

(A) Model depicting developmental progression of thymocytes. Double negative thymocytes can be broken down into four developmental stages based on cell surface expression of CD44 and CD25 as depicted here. (B and C) JE131 cells were infected with the MSCV H2K (Ik-), MSCV Ik-7 H2K (Ik-7), MSCV Ik-1 H2K (Ik-1) or the MSCV p27 GFP (p27) retroviruses. Two to three days post-infection, cells were stained with fluorochrome conjugated anti-H2K antibody, to identify successfully transduced cells, together with antibodies against defined T cell differentiation markers.

cell development. CD25 expression remained high in JE131 cells expressing Ik-7 or no Ikaros (Ik-) and these cells showed no induction of CD4, CD8, CD5, CD69 or TCR expression. However, in JE131 cells expressing Ik-1, CD25 expression dramatically decreased, and CD4, CD8, CD5 CD69 and TCR were upregulated (**Figure 13b, c**). These data suggest that reintroduction of a DNA binding competent isoform of Ikaros (Ik-1) is sufficient to induce a T cell differentiation program in JE131 cells.

To address the role of upregulation of p27 in differentiation of JE131 cells, these experiments were also performed on JE131 cells expressing p27. We found that expression of p27 alone, in the absence of Ikaros, is not sufficient to induce a differentiation program (**Figure 13b**).

Reintroduction of Ik-1 in JE131 cells results in changes in gene expression affecting the cell cycle and upregulation of differentiation markers. These effects could be the result of Ikaros' association with chromatin remodeling complexes, as Ikaros has previously been shown to interact with the NuRD and SWI/SNF chromatin remodeling complexes (26). To address this possibility, acetylation status of histones H3 and H4 was compared in JE131 infected with Ik-1 or control retroviruses (Ik-) by Western blot. Histones were acid extracted from JE131 cells and equal amounts of protein were subjected to SDS-PAGE. A global increase in acetylation was observed on H3 in JE131 cells expressing Ik-1 compared to the control (**Figure 14**). To examine if expression of p27 would result in a similar increase, histones were prepared from JE131 cells expressing p27 and compared to JE131 cells transduced with MSCV retroviruses. We found that the acetylation status of histone H3 in JE131 expressing p27 was lower than JE131 cells alone (**Figure 13**), indicating that expression of p27 alone is not sufficient

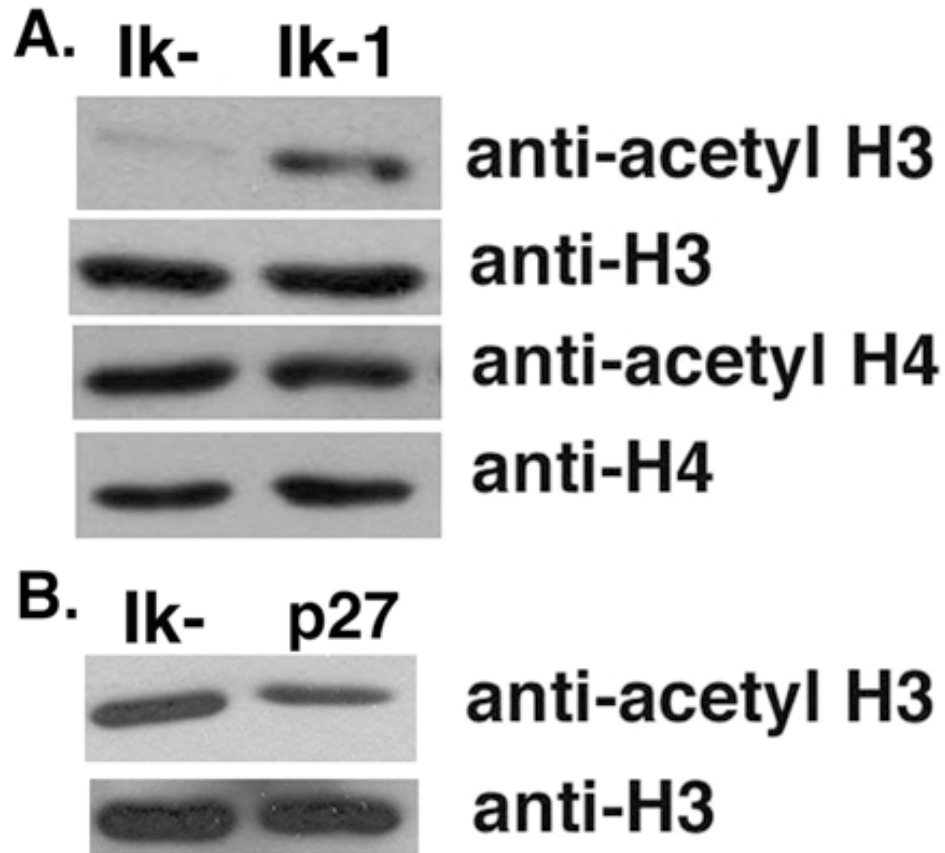


Figure 14. Expression of Ik-1 in JE131 cells induces widespread changes in histone acetylation. JE131 cells were infected with (A) MSCV H2K (Ik-), MSCV Ik-1 H2K (Ik-1) or (B) Ik- or MSCV p27 GFP (p27) retroviruses. Three days post-infection, successfully transduced cells were purified. Histones were prepared using an acid extraction procedure. 10 μ g of protein extract was subjected to SDS PAGE. The blots in panel A and B are representative of six and two independent experiments, respectively. Panel A performed by Angela Minniti Innes and Rachelle Lorenz.

to induce a global increase in histone acetylation in JE131 cells.

Discussion

Tumor suppressor genes encode proteins that, when absent or mutated, result in unregulated growth. Reintroduction of these proteins to null cells often results in reduced growth rates (3). This chapter provides evidence in support of defining Ikaros as a tumor suppressor. Expression of Ikaros in Ikaros null cells leads to growth suppression and cell cycle arrest. These data fulfill part of the definition of a tumor suppressor and, when combined with previous data showing Ikaros deficient mice develop leukemia with 100% penetrance (33, 34), demonstrate that Ikaros fulfills the requirements to be defined as a tumor suppressor.

These data resemble data shown for other tumor suppressors, namely p53 and Wilms Tumor 1 (WT1). In p53 null pre B cells, reintroduction of p53 expression results in growth suppression (107). Glioblastoma and osteosarcoma cell lines with forced p53 expression also demonstrate reduced growth potential (9, 10). The same effect is observed with WT1. Various cell lines undergo growth control and/or growth arrest upon reintroduction of wild type WT1 (19, 20, 108). Our data show that Ikaros functions in the JE131 cells in a manner similar to other tumor suppressors in its ability to repress growth and promote cell cycle arrest, providing evidence that Ikaros is functioning as a tumor suppressor.

Hallmarks of tumor suppressor induced cell cycle arrest include downregulation of cell cycle promoting genes and/or upregulation of cell cycle inhibitor expression. Cyclin E, which promotes cell cycle progression, has been shown to be negatively regulated by WT1 in a myeloid progenitor cell line (18). Reintroduction of p53 in a T cell lymphoma line results in increased

expression of the cell cycle inhibitor, p21 (11). Expression of Ikaros also results in altered expression of an important cell cycle regulator, p27. Expression of p27 increases at both the mRNA and protein levels in JE131 cells expressing Ikaros. We believe the expression of p27 in JE131 cells contributes to the cell cycle arrest observed in these cells, which is supported by the phenotype of the JE131 cells expressing p27, but not Ikaros. These cells undergo a similar reduction in growth potential and cell cycle arrest, suggesting that expression of p27 is important for the observed growth changes in JE131 cells.

p27 expression is controlled at both the protein level, by ubiquitination (109) and transcriptionally, as observed in JE131 cells expressing Ikaros. In vascular endothelial cells, *p27* expression was shown to increase upon Rac1 induction from cell-cell contact (110). In human dermal fibroblasts, repression of expression of the bHLH transcriptional repressor, Inhibitors of Differentiation 3 (Id3), led to an increase in *p27* expression (111). In a mouse pro-B cell line, the forkhead transcription factor FKHR-L1 was shown to transcriptionally regulate *p27* in response to IL-3 (112). These data demonstrate that transcriptional regulation of *p27* is an important part of cell cycle control. It also suggests a role for Ikaros in the regulation of *p27*. There are two possible mechanisms for this regulation. First, Ikaros is a DNA binding transcription factor and may function to directly regulate expression of *p27*. However, luciferase and ChIP assays failed to support this possibility. Second, Ikaros may function further upstream of p27 and may regulate expression of another factor that regulates *p27* expression.

In addition to regulating the cell cycle, reintroduction of p53 and WT1 have also been linked to differentiation. Interference with p53 expression has been shown to inhibit muscle and hematopoietic differentiation (113). Reintroduction of p53 was also shown to promote

differentiation in several acute and chronic leukemia lines (14, 107). WT1 expression in null cells also results in differentiation. Retroviral reintroduction of WT1 to myeloid leukemia cell lines led to cell cycle arrest and differentiation (21). These results are similar to our observed results upon reintroduction of Ikaros to Ikaros null cells. Four days post-infection, T cell differentiation markers were upregulated in JE131 cells expressing Ikaros. These markers suggest a progression by JE131 cells from the double negative (DN) stage to the double positive (DP) stage of the T cell development pathway induced by Ikaros.

p27 expression has also been shown to be important in regulation of differentiation. High expression levels of *p27* have been found in primitive hematopoietic cells, suggesting that *p27* plays a role in maintaining these cells in a quiescent state (114-116). Downregulation of *p27* has been shown to be necessary for further development of T cells in stages that require proliferation (55). More specifically, analysis of *p27* expression in T cell development has shown that *p27* expression is high in early DN thymocytes, then is reduced in late DN, and again restored to high levels at the DP stage (55). This pattern of expression is also observed in JE131 cells. Without Ikaros, JE131 cells express low levels of *p27*, mirroring that observed in late DN thymocytes. Upon Ikaros reintroduction, *p27* expression increases and is followed by upregulation of T cell differentiation markers, mimicking progression to the DP stage. The inability of *p27* expression alone to fully mimic Ikaros activity, however, indicates that changes in *p27* expression are not sufficient to induce differentiation of JE131 cells. This suggests that lack of Ikaros, not reduced levels of *p27*, is necessary for the leukemic phenotype of the JE131 cells.

Ikaros has previously been shown to interact with chromatin remodeling complexes (37). Ikaros expression in JE131 cells results in a global increase of histone H3 acetylation. We observed no increase in histone H3 acetylation in JE131 cells expressing p27, as was seen in JE131 cells expressing Ikaros. This suggests that expression of *p27* alone is not sufficient to induce global changes in histone modifications and that provides evidence that Ikaros expression is required for this to occur.

Overall, our data suggests that Ikaros functions as a tumor suppressor in JE131 cells. Reintroduction of Ikaros in JE131 cells results in cell cycle arrest and upregulation of T cell differentiation markers. Ikaros expression also leads to a global increase in histone H3 acetylation. These data show that Ikaros fulfills the definition of a tumor suppressor.

Chapter IV.

Ikaros directly represses the Notch target gene *Hes1* in JE131 cells

Introduction

In previous studies, we demonstrated that expression of Ikaros in Ikaros null JE131 cells leads to upregulation of *p27* (**Figure 11**). In pursuit of a transcriptional regulator of *p27*, we examined hairy enhancer of split 1, or *Hes1*, as it has been shown to regulate *p27* expression (124). *Hes1* is a basic helix-loop-helix transcription factor that binds to the N box sequence (CACNAG) of its target gene regulatory regions. This inhibits binding of other transcription factors to the adjacent E box (CANNTG), thereby silencing transcription (117). *Hes1* has been shown to be important for development of multiple systems including neuronal development (118, 119), eye morphogenesis (119), expansion of hematopoietic stem cells (120) and T cell development (86, 121). In T cell development, *Hes1* expression has been shown to be critical for proper expansion of thymocytes at various stages of T cell development (86). *Hes1* expression has been shown to be high at the DN3 stage of T cell development, the stage of development where the JE131 cells are arrested, and reduced at the DP stage (122). *Hes1* has also been shown to silence CD4 expression in T cells. Overexpression of *Hes1* in CD4⁺CD8⁻ T cells leads to downregulation of CD4 expression (123). Transcriptional repression of *p27* has also been demonstrated in embryonic carcinoma cells and HeLa cells. In these cells, expression of *Hes1* lead to reduced levels of *p27* at the level of transcription. In addition, *p27* levels were increased in mice lacking *Hes1* (124). These data are striking because we have shown that Ikaros

expression in JE131 cells leads to upregulation of CD4 and *p27* (**Figures 13 and 11**), suggesting possible junction of pathways between Hes1 and Ikaros in regulation of *CD4* and *p27*, perhaps through Ikaros mediated repression of Hes1.

Hes1 has been shown to function downstream of the Notch receptor (125). Notch is a transmembrane protein involved in survival, proliferation and differentiation of many cell types. The Notch receptor is expressed on the cell surface and undergoes two cleavage events upon ligand binding (77). These cleavage events, in part mediated by a presenilin containing γ -secretase complex (78), results in the formation of intracellular Notch, or ICN. ICN then translocates to the nucleus and forms an activation complex with the DNA binding factor, RBP-J κ (RBP-J) and other co-activators (79, 80). This complex activates Notch targets genes through direct DNA binding of RBP-J to the consensus sequence GGGAA (83). Surprisingly, RBP-J shares its DNA binding consensus sequence with Ikaros (25).

Not only do Ikaros and Notch share a DNA binding consensus sequence, they have also been shown to cooperate in leukemogenesis (89, 90, 126). In Notch induced leukemia, proviral insertion in the Ikaros locus was shown to promote a more aggressive disease (89). In mice with a hypomorphic Ikaros mutation in exon 2, inappropriate expression of ICN is observed in leukemic cells (126). Leukemia arising under Notch overexpression resembles that observed upon loss of Ikaros because in both cases, leukemia is specific for the T cell lineage, arises within thymocyte population, and requires pre-TCR or TCR signaling (33, 34, 91). Notch (53, 73) and Ikaros (62, 64, 127) have also been shown, albeit separately, to be critical for proper T cell development. When taken together, these data suggest a role for Ikaros in regulation of Notch signaling.

Results

Restoration of Ikaros results in down-regulation of *Hes1* expression

The bHLH transcription factor, *Hes1*, has previously been shown to repress expression of the T cell differentiation marker, *CD4*, and the cell cycle regulator, *p27kip1* (*p27*) (123, 124, 128). Interestingly, we showed that reintroduction of Ikaros to the JE131 Ikaros null T leukemia cell line leads to upregulation of both *CD4* and *p27* (**Figures 13 and 11**). Therefore, we postulated that in JE131 cells that lack expression of Ikaros, *Hes1* expression levels in JE131 cells would be elevated. We hypothesized that the up-regulation of *CD4* and *p27kip1* in JE131 cells transduced with Ikaros may be the result of reduced expression of *Hes1* in the presence of Ikaros. Reduction in *Hes1* expression would relieve *Hes1*-induced repression of *CD4* and *p27*. To begin to address this possibility, *Hes1* expression was analyzed in JE131 cells transduced with the Ikaros isoform, Ik-1 (Ik-1) or the negative control retrovirus (Ik-). RNA was prepared from JE131 cells not expressing Ikaros and those expressing Ik-1 and subjected to semi-quantitative RT-PCR with primers for *HPRT* and *Hes1*. *p27* was used as a positive control, since we have previously shown changes in its expression in the presence of Ikaros (**Figure 11**). RT-PCR results showed that JE131 cells without Ikaros have high expression levels of *Hes1*. JE131 cells transduced with Ik-1, however, displayed a dramatic down-regulation of *Hes1* expression (**Figure 15**).

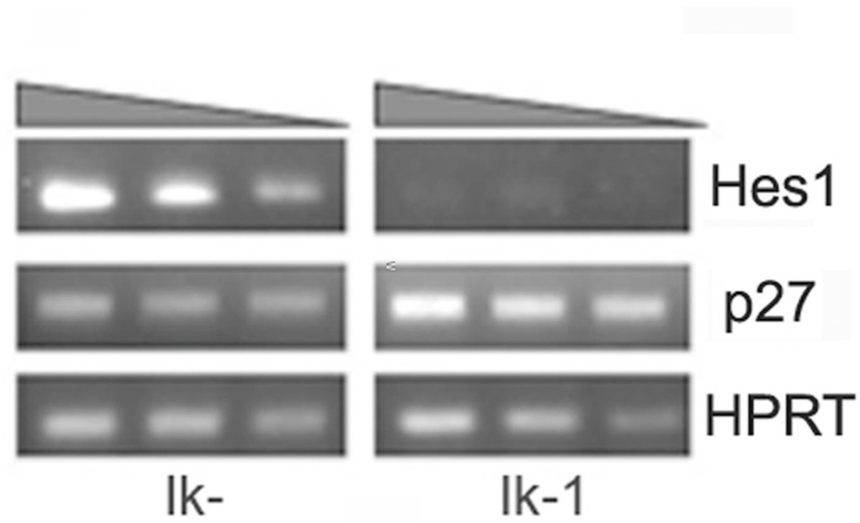


Figure 15. The Notch target gene, *Hes1*, is repressed upon reintroduction of *Ik-1* to JE131 cells. Twenty-four hours post-infection, JE131 cells successfully infected with MSCV H2K (*Ik-*) or MSCV *Ik-1* H2K (*Ik-1*) retroviruses were purified using H2K as a marker of successful transduction. cDNA was prepared and analyzed by semi-quantitative RT-PCR. Expression of *Hes1*, *p27kip1*, and the housekeeping gene *HPRT* in each population is shown. The shaded triangle above the blots indicates decreasing amounts of cDNA.

Treatment with γ -secretase inhibitor has minimal effect on proliferation of JE131 cells

Hes1 has previously been identified as a Notch target gene and Notch signaling up-regulates *Hes1* expression (129). By Western blot, we found that the activated form of Notch, ICN, was present in the JE131 cells (**Figure 16**). This suggests that the high *Hes1* expression in JE131 cells may result from activated Notch signaling in these cells. These results led us to examine the role of ICN in the JE131 cells.

To determine if generation of ICN was essential for viability and/or proliferation of JE131 cells, the pharmacological γ -secretase inhibitor (GSI), *N*-[*N*-(3,5-difluorophenacetyl)-L-alanyl]-*S*-phenylglycine *t*-butyl ester (DAPT) was utilized. DAPT blocks the γ -secretase mediated cleavage of Notch through binding to the C terminal fragment of presenilin, thus preventing formation of ICN and its translocation to the nucleus (130). Previous studies have shown that addition of GSI to rapidly growing mouse leukemia cell lines that express ICN frequently can result in G0/G1 arrest and apoptosis (126, 131). In particular, 5 μ M DAPT has been shown to be sufficient to induce cell cycle arrest and apoptosis in murine T-ALL cell lines with activating Notch1 mutations (131). However, in the JE131 cells, addition of 5 μ M or 1 μ M DAPT to the culture medium resulted in only a minimal effect on the cells' ability to proliferate compared to the DMSO control populations (**Figure 17a**).

To confirm the efficiency of DAPT treatment in preventing ICN cleavage, ICN levels were measured by Western blot analyses using protein extracts prepared from JE131 cells after five days in culture with DAPT or DMSO. An antibody that specifically recognizes Notch cleaved at valine 744 was utilized to detect ICN and not all forms of Notch. In DAPT treated cells, a decrease in levels of ICN was observed compared to the DMSO treated controls

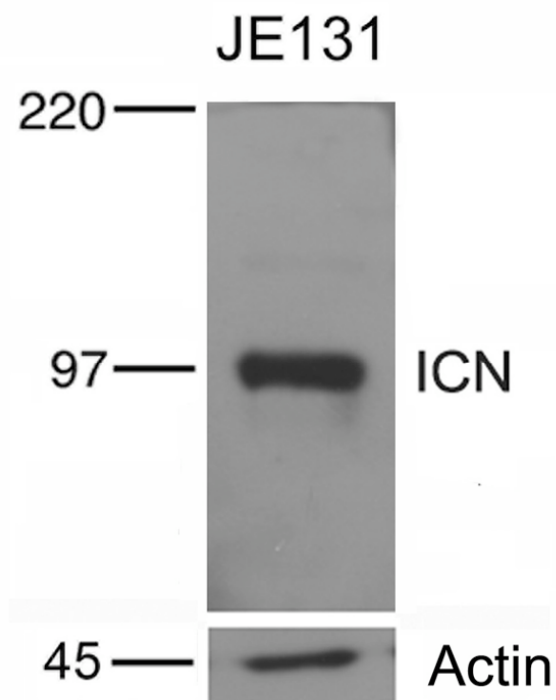
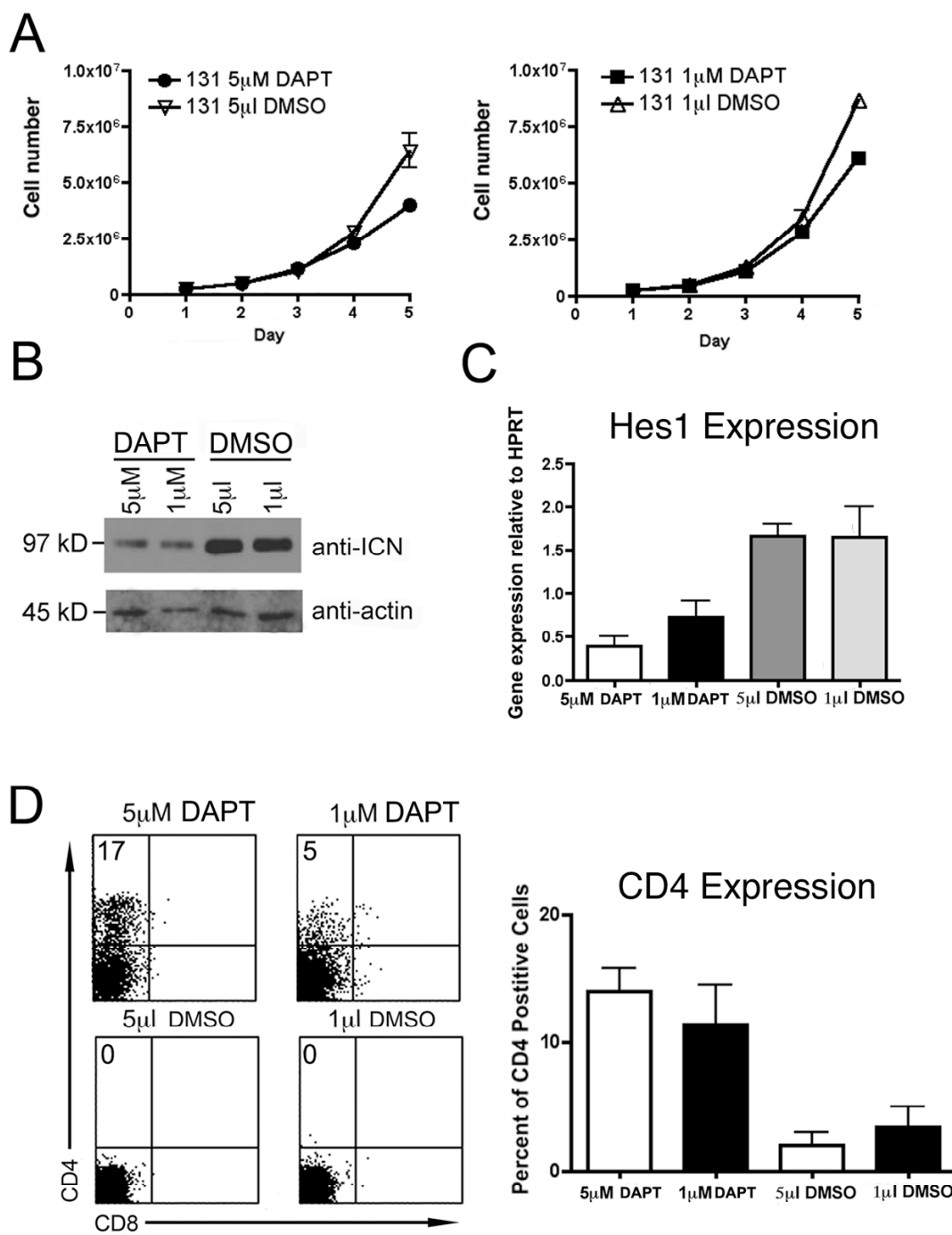


Figure 16. JE131 cells contain intracellular Notch (ICN). Western blot analysis of JE131 whole cell extracts. Blots were probed with antibodies directed against intracellular Notch1 (ICN) that has been properly cleaved at val1744. Blots were also probed with anti-actin antibodies as a loading control. Blot performed by Sheila Chari.

Figure 17. The γ -secretase inhibitor, DAPT, has minimal effects on growth of JE131 cells, but leads to upregulation of CD4. (A) 2.5×10^5 JE131 cells were cultured with 5 μ M DAPT, 1 μ M DAPT, 5 μ l DMSO or 1 μ M DMSO in a 24 well plate. Counts of viable cells were performed every 24 hours. Graphs depict results of two experiments with error bars (+/- standard deviation). (B) Western blot analysis of 30 μ g/lane of protein extracts prepared from JE131 cells treated with 5 μ M DAPT, 1 μ M DAPT, 5 μ l DMSO or 1 μ M DMSO for 4 days. Blots were probed with antibodies directed against intracellular Notch1 (ICN) that has been properly cleaved at val1744. Blots were also probed with anti-actin antibodies as a loading control. (C) qRT-PCR analyses of *Hes1* expression were performed using cDNA prepared from JE131 cells treated with 5 μ M DAPT, 1 μ M DAPT, 5 μ l DMSO or 1 μ l DMSO. Y-axis shows gene expression normalized to expression of the housekeeping gene, *HPRT*. Values were determined by the Pfaffl method and are shown as ratios ($2^{-\Delta CT_{\text{target}}}:2^{-\Delta CT_{\text{reference}}}$). Target = gene of interest; reference = *HPRT*. Bar graph depicts results of two experiments performed in duplicate with error bars (+/- standard deviation). (D) JE131 cells treated with 5 μ M DAPT, 1 μ M DAPT, 5 μ l DMSO or 1 μ l DMSO for 4 days were stained with fluorochrome-conjugated antibodies against CD4 and CD8. Representative flow cytometric dot plots are shown. Bar graph depicts results of three experiments with error bars (+/- standard deviation).



(**Figure 17b**). Therefore, high levels of ICN are not required for viability and proliferation of JE131 cells. This is in contrast to JE131 cells transduced with Ikaros, which undergo rapid cell cycle arrest (**Figure 6**), suggesting that the proliferative capacity of JE131 cells is primarily dependent upon lack of Ikaros rather than generation of ICN.

Reduction of ICN levels leads to reduced expression of *Hes1* and up-regulation of the T cell differentiation marker, CD4

To verify that the reduction observed in levels of ICN in JE131 cells was sufficient to affect Notch target gene expression, *Hes1* expression was analyzed in the presence and absence of DAPT in JE131 cells. Quantitative RT-PCR (qRT-PCR) was performed on cDNA generated from JE131 cells treated with DAPT or DMSO (negative control). Treatment of JE131 cells with DAPT led to a decrease in *Hes1* expression compared to that observed in cells treated with DMSO (**Figure 17c**). Therefore, the DAPT induced reduction in ICN levels was sufficient to diminish *Hes1* expression in JE131 cells, even though proliferation was unaffected.

The phenotype of the JE131 cells, CD4-CD8-TCR-CD44-CD25⁺, places them at the DN3 stage of T cell development. Reintroduction of Ikaros in these cells induces a T cell specific program of gene expression in which expression of T cell differentiation markers such as CD4 and CD8 are upregulated (**Figure 13**). Since *Hes1* has been implicated in repression of *CD4* (123, 128) and DAPT reduces *Hes1* levels, we hypothesized that JE131 cells grown in the presence of DAPT may up-regulate CD4 in a manner similar to JE131 cells expressing Ikaros. To test this, JE131 cells were cultured in the presence of 5 μ M or 1 μ M DAPT or the equivalent amount of DMSO and stained with antibodies against CD4 and CD8 after 4 days in culture. We

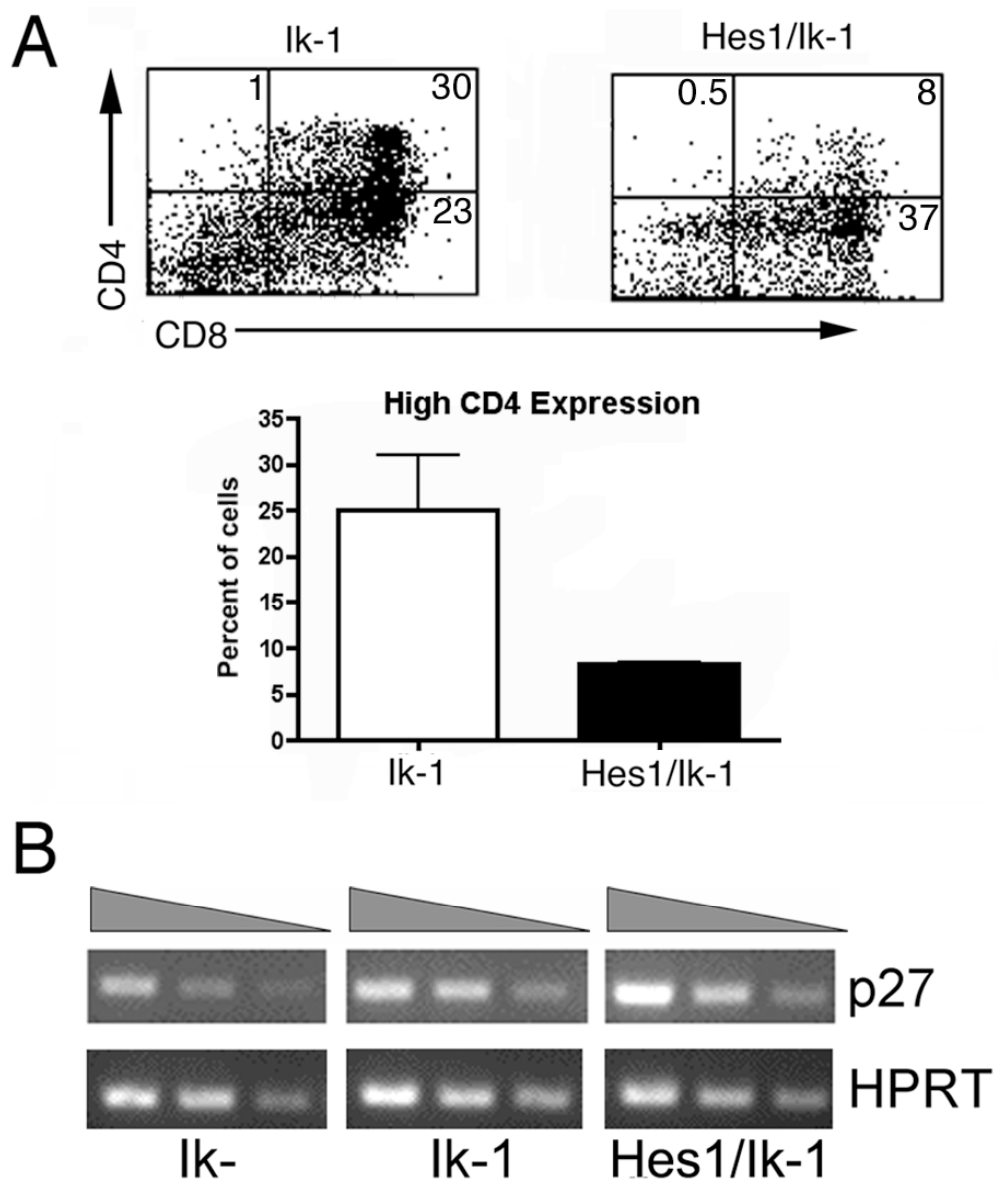
found that JE131 cells treated with DAPT up-regulate CD4, but not CD8 (**Figure 17d**). These data suggest that inactivation of Notch signaling is sufficient to induce CD4 expression in JE131 cells, even in the absence of Ikaros. Note that this is not the case for CD8 (**Figure 17d**).

Forced expression of *Hes1* in the presence of Ikaros interferes with high-levels of induced CD4 expression

In JE131 cells, reintroduction of Ikaros and treatment with DAPT both result in up-regulation of CD4 (**Figure 13d and 17d**) and down-regulation of *Hes1* (**Figures 15 and 17c**), indicating that in Ikaros transduced JE131 cells, CD4 up-regulation may result from repression of *Hes1* by Ikaros. We hypothesized that expression of *Hes1* in the presence of Ikaros would obscure the effect of Ikaros on *Hes1* expression, thereby preventing the downstream effects of repression of *Hes1*. To address this possibility, JE131 cells were co-transduced with *Hes1* and Ikaros (Ik-1) to force continued high-level expression of *Hes1* in the presence of Ikaros, where it would normally be down-regulated. In co-transduced JE131 cells, altered expression levels of CD4 were observed compared to JE131 cells transduced with Ikaros alone. More specifically, co-transduction with *Hes1* decreased Ikaros' ability to induce high-level expression of CD4 (**Figure 18a**). These data provide evidence that up-regulation of CD4 observed in Ikaros-transduced JE131 cells is partially induced by Ikaros-driven repression of *Hes1*.

Hes1 has been implicated as a repressor of *p27kip1*, and *p27kip1* levels increase upon expression of Ikaros in the Ikaros null JE131 cells (**Figure 11**). Therefore, Ikaros-induced up-regulation of *Hes1* may be the mechanism behind up-regulation of *p27kip1* in Ikaros-transduced JE131 cells. To examine this possibility, expression levels of *p27kip1* were analyzed in JE131

Figure 18. Preventing down-regulation of *Hes1* decreases Ikaros' ability to induce high-level expression of CD4. (A) JE131 cells were infected with MSCV GFP and MSCV Ik-1 H2K (Ik-1) or MSCV Hes-1 GFP and MSCV Ik-1 H2K (Hes1/Ik-1) retroviruses, and sorted for H2K expression using magnetic beads. Four days post-infection, cells were stained with fluorochrome-conjugated antibodies against CD4 and CD8. Flow cytometric dot plots depict CD4 and CD8 staining for GFP positive cells in each culture. "High" CD4 expression appears in the upper right and upper left quadrants of each plot. Percentages of cells that fall into each quadrant are shown. Bar graph depicts results of two experiments with error bars (+/- standard deviation). (B) Semi-quantitative RT-PCR analysis of *p27kip1* expression was performed using cDNA from JE131 transduced with Ik-, Ik-1 or Ik-1 and Hes1 retroviruses. Twenty-four hours post infection, JE131 cells were purified using H-2Kk and GFP as markers of successful transduction. cDNA was prepared and analyzed. Expression of *p27kip1* and the housekeeping gene, *HPRT*, are shown for each population. The shaded triangle above the blots indicates decreasing amounts of cDNA.



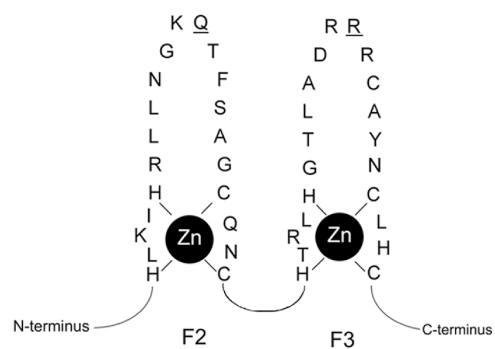
cells transduced with Ikaros and Hes1 retroviruses by semi-quantitative RT-PCR using primers for *p27kip1* and *HPRT* as the control housekeeping gene. *p27kip1* expression levels were unaffected in the presence of Ikaros and Hes1 compared to Ikaros alone (**Figure 18b**). Thus, *Hes1* repression by Ikaros does not contribute to the up-regulation of *p27kip1* in JE131 cells transduced with Ikaros.

Repression of *Hes1* expression requires Ikaros' sequence-specific DNA binding ability

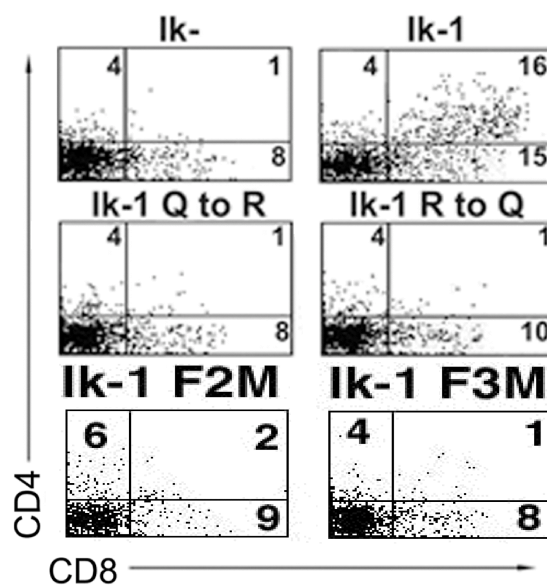
Four mutations in the F2 and F3 zinc fingers in Ikaros were generated to address the requirement for DNA binding ability of Ikaros in repression of *Hes1* and upregulation of differentiation markers. First, point mutations were generated in the F2 (IkF2M) and F3 (IkF3M) zinc fingers. These mutations prevent Zn binding, so zinc finger formation is completely disrupted. The second set of mutations does not disrupt zinc finger formation, but abrogates Ikaros' ability to bind at its sequence-specific DNA binding site, as the mutations alter one of the DNA binding amino acids in each finger, (F2, Ik Q to R; F3, Ik R to Q) (**Figure 19a**) (46). These subtle mutations preserve Ikaros' tertiary structure and, therefore, would be highly unlikely to affect its ability to interact with other proteins, but disrupt Ikaros' ability to bind to the sequence GGGAA (46) (**Figure 19a**). MSCV Ik-1 H2K was subjected to site directed mutagenesis by overlap extension (SOE) with primers that included the desired mutation in either the F2 or F3 zinc finger (132). These mutant Ikaros constructs were then used to generate retroviruses to infect JE131 cells and cells were stained with antibodies against CD4 and CD8. All four mutations prevented Ikaros-induced up-regulation of CD4 and CD8 (**Figure 19b**). Furthermore, the two DNA binding region specific mutations rendered Ikaros completely unable

Figure 19. DNA binding specificity is required for Ikaros' ability to repress *Hes1*. (A) Point mutations that abrogate Ikaros' ability to bind to its consensus DNA binding site, GGGAA, were generated by site-directed PCR mutagenesis. The mutated DNA bases within the second and third N-terminal zinc fingers (F2 and F3) are underlined. (B) JE131 cells were transduced with Ikaros DNA binding deficient mutants (Ik-1 Q to R, Ik-1 R to Q, Ik-1 F2M, and Ik-1 F3M) and stained with fluorochrome-conjugated antibodies against H2K, CD4 and CD8 four days post-infection. (C) *Hes1* expression was analyzed in JE131 cells transduced with Ikaros DNA binding deficient mutants by qRT-PCR. Twenty-four hours post-infection, H-2Kk positive JE131 cells were purified and cDNA prepared. Expression level for each population is normalized to *HPRT* expression. Bar graph depicts results of two experiments with error bars (+/- standard deviation).

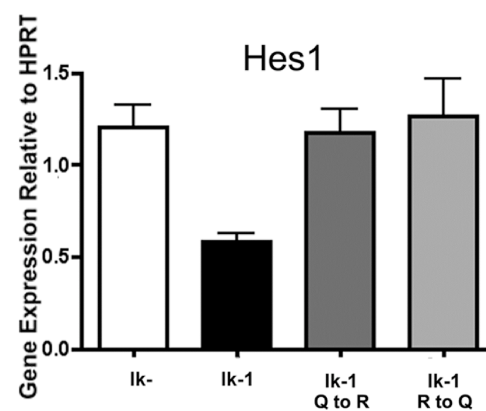
A



B



C

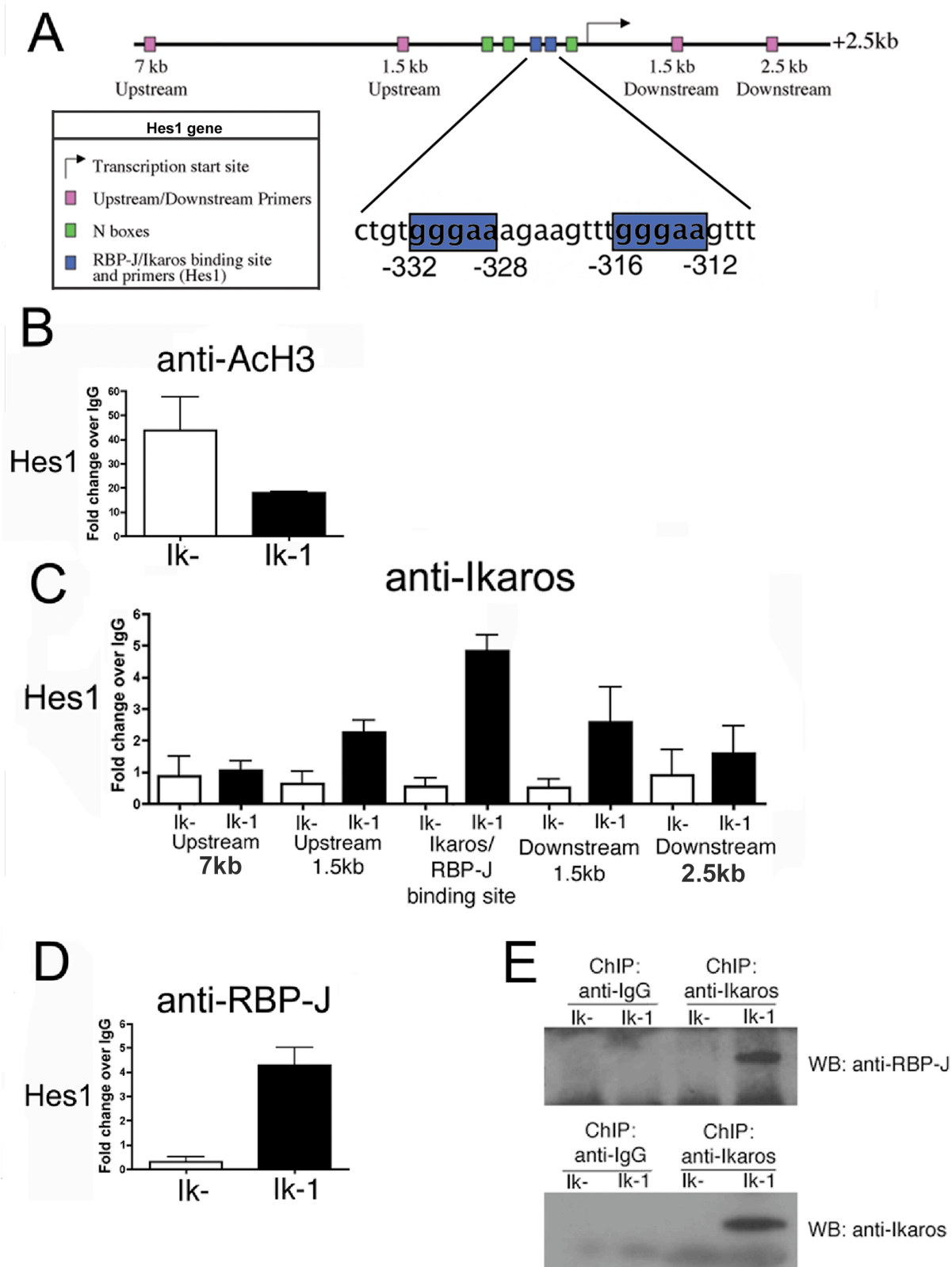


to repress *Hes1* expression, as shown by qRT-PCR performed on cDNA generated from JE131 cells expressing the mutant Ikaros proteins (**Figure 19c**). These data indicate that the F2 and F3 zinc fingers are critical for Ikaros to function in inducing differentiation markers and that down-regulation of *Hes1* expression in JE131 cells transduced with Ikaros occurs through sequence-specific DNA binding of Ikaros.

Hes1 promoter region is deacetylated in the presence of Ikaros

Ikaros participates in chromatin remodeling as a component of both activating and repressing chromatin remodeling complexes. These complexes facilitate chromatin modification, thereby altering accessibility of DNA to transcription factors. Some of these complexes are associated with enzymes, histone acetyltransferases (HATs) and histone deacetyltransferases (HDACs), which alter chromatin formation by addition or removal of acetyl groups, respectively. Ikaros is believed to target these complexes to specific gene loci (37). Repression of *Hes1* expression in JE131 cells transduced with Ikaros may occur through Ikaros' ability to target chromatin remodeling complexes to the *Hes1* promoter. To determine the chromatin state of the *Hes1* promoter, chromatin immunoprecipitation (ChIP) assays were performed on chromatin prepared from JE131 cells transduced with the control retrovirus (Ik-) or Ikaros (Ik-1) using an antibody against acetylated histone H3 (AcH3). AcH3 was chosen because Ikaros has previously been shown to cause a widespread change in histone H3 acetylation in JE131 cells (**Figure 14**). Using real-time quantitative PCR (qPCR) analysis of ChIP DNA, a decrease in acetylation of histone H3 at the *Hes1* promoter was observed in Ikaros transduced JE131 cells as compared to those not expressing Ikaros (**Figure 20b**). These

Figure 20. Ikaros and RBP-J κ bind to the regulatory region of *Hes1*. (A) *Hes1* promoter region with RBP-J κ /Ikaros binding sites are shown in blue boxes. (B, C, D) Chromatin immunoprecipitations (ChIP) with antibodies against acetylated histone H3 (anti-AcH3) (B), Ikaros (anti-Ikaros) (C) or RBP-J κ (anti-RBP-J) (D) were performed on chromatin prepared from populations of JE131 cells successfully transduced with the MSCV retrovirus (Ik-) or the MSCV Ik-1 H2K (Ik-1) retrovirus twenty-four hours post-infection. Analyses of ChIP DNA were performed using qPCR with primers surrounding Ikaros and/or RBP-J κ (RBP-J) binding sites in the upstream regulatory region of *Hes1*. All ChIP analyses were performed with two independent chromatin preparations with at least two immunoprecipitations per chromatin prep. Bar graphs depict results of these two experiments with error bars (+/- standard deviation). (E) ChIP was performed using chromatin prepared from H2K positive JE131 cells that had been infected with Ik- or Ik-1 retroviruses. Control IgG or anti-Ikaros monoclonal antibodies were utilized for immunoprecipitation of the chromatin. Complexes were eluted from beads using Laemmli buffer and Western blot analyses performed using anti-RBP-J (top blot) or anti-Ikaros (bottom blot) antibodies. Stars indicate specific bands. Experiment was performed twice and representative experiment is shown.



data suggest that the presence of Ikaros in JE131 cells represses *Hes1* expression by facilitating changes in histone acetylation at the *Hes1* locus.

Ikaros binds to *Hes1* regulatory regions *in vivo*

To demonstrate direct Ikaros regulation of *Hes1*, Ikaros ChIP experiments were performed. Since it has been shown that Ikaros and RBP-J, the Notch inducible transcriptional activator, can bind the same DNA sequences in electrophoretic mobility shift assays (EMSAs) (126) primers were generated to the *Hes1* regulatory region containing the identified RBP-J binding site (**Figure 20a**). Interestingly, this region contains two consensus Ikaros/RBP-J binding sites (GGGAA) in a head-to-tail configuration. Chromatin was prepared from JE131 cells that had been transduced with Ikaros (Ik-1) as well as those transduced with the control retrovirus (Ik-), and ChIP was performed with anti-Ikaros antibodies. In this way, it was determined that Ikaros binds directly within the *Hes1* regulatory region that has been shown to bind RBP-J (**Figure 20c**).

Although the binding site for RBP-J within *Hes1* has been firmly established by EMSA (125), ChIP (with ICN) (133) and reporter assays (134), this is not the case for Ikaros. Therefore, we tested two additional primer pairs on each side of the Ikaros binding region within *Hes1* (**Figure 20a**). A peak of Ikaros binding was observed within the regulatory region that also contains the RBP-J binding site (**Figure 20c**).

Ikaros and RBP-J bind to DNA simultaneously, not antagonistically

It has been hypothesized that since Ikaros and RBP-J share the same DNA binding consensus sequence, they bind competitively (Beverly, 2003). If RBP-J and Ikaros compete for binding within *Hes1* regulatory sequences, then RBP-J binding within these sequences should be reduced in the presence of Ikaros. To test this hypothesis, RBP-J binding was examined by ChIP analyses with anti-RBP-J antibodies using chromatin prepared from JE131 cells transduced with Ikaros (Ik-1) or the control retrovirus (Ik-). We surveyed the same consensus Ikaros/RBP-J sites in the regulatory region of *Hes1* as described above to determine if the presence of Ikaros negatively affected levels of RBP-J binding. RBP-J and Ikaros were both detected bound to the *Hes1* regulatory region in JE131 cells transduced with Ik-1 (**Figure 20d**). Surprisingly, RBP-J binding to the *Hes1* promoter did not decrease, but actually increased in the presence of Ikaros. In fact, RBP-J binding was undetectable unless Ikaros was also expressed (**Figure 20d**).

As a further test to determine if Ikaros and RBP-J bind DNA concomitantly, ChIP was performed followed by Western blot analyses. Chromatin prepared from Ikaros-transduced JE131 cells was immunoprecipitated with anti-Ikaros antibodies, followed by Western blot analyses of the protein component of the immunoprecipitate using anti-RBP-J and anti-Ikaros antibodies. Anti-Ikaros antibodies precipitated chromatin fragments that contained both Ikaros and RBP-J (**Figure 20e**). Thus, these data confirm that Ikaros and RBP-J can bind together within small regions of chromatin, supporting our model of concurrent and not antagonistic binding.

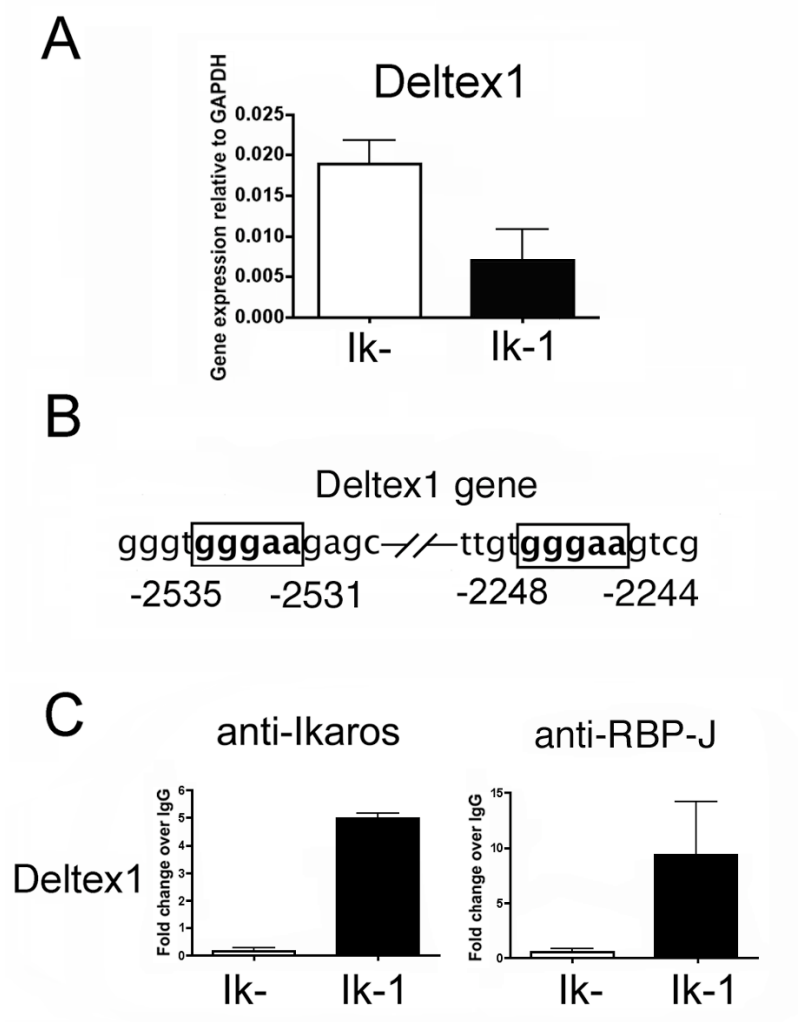
Ikaros' role as a direct repressor of Notch target genes extends to *Deltex1*

To determine if this mode of regulation extends to other Notch target genes, we investigated whether Ikaros could bind within potential regulatory sequences of the Notch target gene, *Deltex1*. *Deltex1* encodes a putative E3-ubiquitin ligase whose expression is highly induced by Notch signals in thymocytes (135).

Expression levels of *Deltex1* were compared by qRT-PCR in JE131 cells transduced with Ikaros (Ik-1) or control retroviruses (Ik-). Compared to JE131 cells not expressing Ikaros, *Deltex1* expression decreased upon reintroduction of Ikaros to JE131 cells (**Figure 21a**). Although *Deltex1* expression is frequently used as a marker for Notch activation, its regulatory elements have not been well defined. Therefore, we scanned sequences upstream of the *Deltex1* transcriptional start site for potential RBP-J/Ikaros binding sites using the UCSC Genome Browser. Two such sites were defined, within region -1782 to -1491 relative to the start site of transcription (**Figure 21b**).

ChIP was performed with anti-Ikaros antibodies and chromatin prepared from JE131 cells transduced with Ikaros (Ik-1) or the control retrovirus (Ik-). Binding of Ikaros to *Deltex1* was observed in the proposed Ikaros binding region of the *Deltex1* gene, suggesting that Ikaros directly represses *Deltex1* expression by binding to its regulatory regions (**Figure 21c**). ChIP was also performed with anti-RBP-J antibodies on chromatin from JE131 cells transduced with Ik-1 or Ik-. As with the *Hes1* promoter region, RBP-J was detected within the *Deltex1* regulatory region only in presence of Ikaros (**Figure 21c**). These data suggest a global role for Ikaros in the repression of Notch target gene expression.

Figure 21. Ikaros and RBP-J κ bind to the regulatory regions of *Deltex1*. (A) qRT-PCR analysis of *Deltex1* expression in sorted JE131 cells transduced with MSCV H2K (Ik-) or MSCV Ik-1 H2K (Ik-1). Bar graph depicts results of two experiments performed in duplicate with error bars (+/- standard deviation). (B) *Deltex1* sequences with RBP-J/Ikaros binding sites shown in boxes. (C) Chromatin immunoprecipitations (ChIP) were performed on H2K positive JE131 cells twenty-four hours post-infection with the Ik- or Ik-1 retrovirus using antibodies against Ikaros (anti-Ikaros) or RBP-J κ (anti-RBP-J). qPCR analyses of ChIP DNA were performed with primers surrounding Ikaros and/or RBP-J κ (RBP-J) binding sites in upstream regulatory regions of *Deltex1*. ChIP analyses were performed with two independent chromatin preparations with at least two immunoprecipitations per chromatin prep. Bar graph depicts results of these two experiments with error bars (+/- standard deviation).



Discussion

Cooperative mutations in proto-oncogene and tumor suppressor genes occur in many forms of cancer (e.g. colon cancer, pancreatic cancer, melanoma, acute leukemia (136-139). Strong evidence indicates that loss of Ikaros, a tumor suppressor gene, and constitutive activation of Notch1, a proto-oncogene, fits this paradigm in the genesis of T-acute lymphoblastic leukemia (T-ALL) (89, 90, 126, 140). It is likely, therefore, that Ikaros and Notch signaling also intersect in regulation of normal T cell development. Here, we provide evidence for a unique role for Ikaros in direct repression of Notch target genes, by focusing our studies on the role of Ikaros in repression of the canonical Notch target gene, *Hes1*.

In the JE131 T cell line, Ikaros is required for repression of *Hes1*. Notably, downregulation of *Hes1* has been shown to be important for progression of T cell development, specifically at the DN3 stage (86). Our data suggest a role for Ikaros in the progression of T cell development through downregulation of *Hes1* expression. JE131 cells are arrested at the DN3 stage and express high levels of *Hes1*. Ikaros reintroduction results in *Hes1* downregulation, ultimately resulting in a T cell differentiation program resembling the DP stage. This transitional change in gene expression pattern is similar to that observed in thymocytes transitioning from DN to DP cells (86). *Deltex1* and *Notch1* expression also decrease upon transition from DN to DP (122), which observe in the JE131 cells transduced with Ikaros. Taken together, these data suggest that regulation of Notch target genes by Ikaros is essential for proper transition from the DN to DP stages in T cell development.

Three explanations for the downregulation of Notch target genes were evaluated. The first possibility was that Ikaros might interact with a factor necessary for induction of Notch target

gene expression (i.e. Mastermind-like), thereby sequestering it from interacting with RBP-J until Notch/Notch-ligand interactions occur. To test this possibility, point mutations were introduced that would alter Ikaros' sequence-specific DNA binding ability without affecting its tertiary structure. These point mutations abrogated Ikaros' ability to downregulate *Hes1*, suggesting that DNA binding is necessary for downregulation of *Hes1*, making this possibility unlikely. Secondly, Ikaros may compete for binding with RBP-J and function as a more efficient repressor of Notch target genes. However, evidence was provided that Ikaros and RBP-J are both bound to regulatory elements of *Hes1* and *Deltex1* when these genes are repressed. In addition, Ikaros and RBP-J co-immunoprecipitated, as shown in the ChIP western. These data suggest that the competitive binding mechanism is also incorrect. The third, and we suggest the correct mechanism, is that Ikaros and RBP-J bind simultaneously to the regulatory regions of *Hes1* and *Deltex1*. These data provide evidence, for the first time, that RBP-J may require the presence of another DNA binding factor, in this case Ikaros, in order to efficiently repress gene expression. A precedent exists for functional interaction of RBP-J and zinc finger DNA binding proteins in Notch gene regulation, albeit in gene activation, not repression as we show here. It has been suggested that the Notch protein, Notch 3, requires binding of a zinc finger DNA binding protein in conjunction with RBP-J for Notch gene activation (141), although it is unknown, to date, how these two proteins function together.

We hypothesize that the role of Ikaros in Notch target gene repression may be to stabilize interaction of components of the co-repressor complex (i.e. histone deacetylase activity) to regulatory elements bound by RBP-J or to facilitate changes in DNA structure which allow more efficient RBP-J DNA binding. Both Ikaros and RBP-J have been shown to interact with

components of chromatin remodeling complexes, including HDAC and CtBP, providing a potential mechanism for this interaction (46, 49, 81, 82). Within the *Hes1* promoter, there are two RBP-J/Ikaros sites in close proximity. Therefore, Ikaros and RBP-J may each bind to one of these sites where the associated chromatin remodeling complexes form a bridge between the Ikaros and RBP-J (**Figure 22**). It is also possible that only Ikaros binds to the sites and RBP-J may be a component of the repressive complex or that Ikaros may bind first and remodel the chromatin so that RBP-J can then bind (**Figure 22**).

We hypothesize that this is also the case for the two consensus Ikaros/RBP-J binding sites in *Deltex*. In the case of *Deltex*, however, the two sites are farther apart than those observed in *Hes1*. Interestingly, the distance separating them, 291 bp, corresponds almost exactly with two turns of the DNA around the nucleosome ($146 \text{ bp/turn} \times 2 = 292 \text{ bp}$), which places them in closer vicinity in three-dimensional space than would be expected from the linear DNA sequence.

It cannot yet be explained why robust RBP-J binding to *Hes1* and *Deltex1* regulatory regions was only observed when Ikaros was present. One possibility is that when RBP-J is in the context of a co-activator complex in T lymphocytes, the epitopes for the immunoprecipitating antibodies are not accessible. Nevertheless, it is evident from the data presented here that Ikaros and RBP-J bind together to facilitate repression of *Hes1*. This cooperation extends to another Notch target gene, *Deltex1*, suggesting it may be a more universal mechanism for Notch target gene repression in developing T cells.

Previous data (**Figure 14**) showed that expression of Ik-1 in JE131 cells led to a global increase in histone acetylation on histone H3. However, Ikaros regulation of *Hes1* defines a role for Ikaros in repression through deacetylation (**Figure 20b**). Interestingly, though, both direct

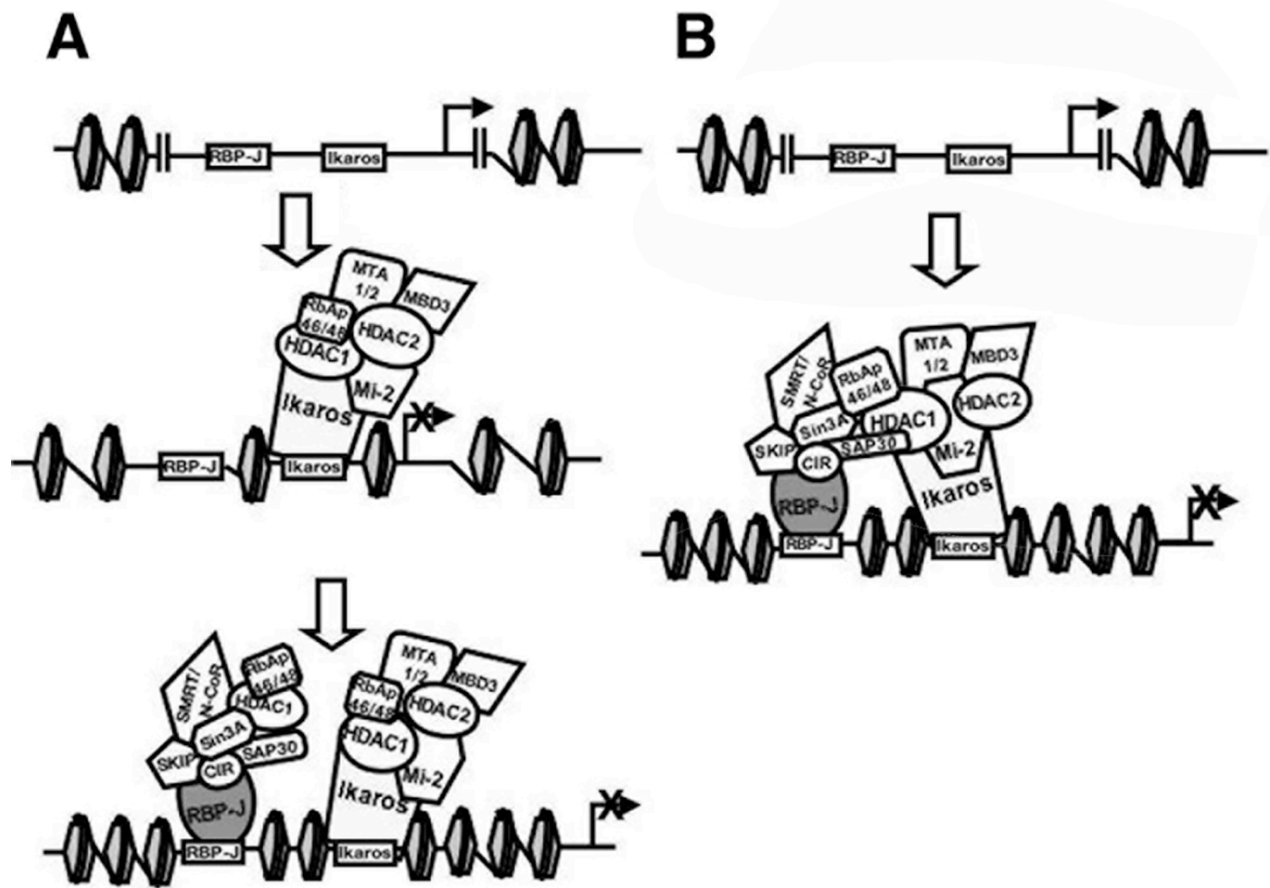


Figure 22. Two hypotheses for cooperative DNA binding of Ikaros and RBP-J κ during gene repression. (A) Ikaros binding is required to alter chromatin structure, thereby facilitating RBP-J κ (RBP-J) binding to DNA. (B) Ikaros (or its interacting proteins) interacts directly with RBP-J κ (or its interacting proteins) on the DNA, thereby stabilizing interactions of RBP-J κ with the DNA.

targets of Ikaros, Hes1 and Deltex1, have been shown to function, at least in part, as repressors (75). It is intriguing to hypothesize that Ikaros may be repressing the activity of multiple proteins that function as repressors. De-repression of target genes could then lead to expression of these genes. Ikaros repression of Hes1, for example, leads to CD4 expression. Ikaros repression of the repressor Hes1 results in gene expression of CD4. Ikaros mediated repression of repressor proteins could then result in an increase in expression of downstream targets and would explain the increase in acetylation.

We contend that lack of Ikaros results in de-repression, as opposed to activation, of Notch target genes. Therefore, constitutive generation of ICN in Ikaros deficient cells may further increase expression of de-repressed Notch target genes. This is likely the mechanism behind cooperative Ikaros loss-of-function mutations that were identified in ICN-induced leukemia in mice, which significantly accelerated disease course (89). Interestingly, both activating mutations in Notch1 and aberrant Ikaros expression have been described in human T-ALL (142, 143). The importance of high level ICN expression to viability of human leukemia cells has been demonstrated through the use of γ -secretase inhibitors (GSIs). Some, but not all, T-ALL with activating Notch mutations are sensitive to treatment with GSIs, displaying apoptosis and/or growth arrest (87). A recent report has demonstrated that GSI decreases growth of a leukemia cell line arising in a mouse with a hypomorphic Ikaros allele (126). However, we demonstrate that the JE131 cell line is refractory to treatment with GSI, showing that it is not dependent on ICN for viability and proliferation. It could be suggested that this is the result of cumulative mutations that have arisen in these cells over time in culture. However, it must be emphasized that growth of JE131 cells can still be dramatically and consistently slowed through restoration

of Ikaros by retroviral transduction (**Figure 6**). These data suggest that viability and proliferative capacity of JE131 cells is driven predominantly by their lack of Ikaros rather than constitutive generation of ICN. It is likely that the relative contribution of lack of Ikaros and constitutive ICN generation to viability will differ from leukemia to leukemia.

These studies began with the observation that re-introduction of Ikaros into JE131 Ikaros null leukemia cells promotes up-regulation of the T cell differentiation marker, CD4 and the cell cycle regulator, p27. We initially hypothesized that down-regulation of *Hes1* may underlie up-regulation of *CD4* and *p27* in Ikaros transduced JE131 cells, since *Hes1* is a common factor reported to be involved in their regulation (123, 124, 128). We demonstrate that forced expression of *Hes1* in Ikaros-transduced cells can interfere with the ability of Ikaros to induce high-level expression of CD4, suggesting that *Hes1* down-regulation by Ikaros does indeed contribute to Ikaros' ability to initiate high-level CD4 expression in these cells. These data also provide evidence for a role for *Hes1* in fine-tuning levels of CD4 gene expression in developing thymocytes. The *Runx1* and *Runx3* transcriptional repressors, known to be critically important for *CD4* silencing, are also Notch target genes (144-146) and could also contribute to the mechanism behind Ikaros' positive role in regulation of CD4 expression. We did not observe any changes in *p27* expression in JE131 cells transduced with both *Hes1* and Ikaros, suggesting that *Hes1* by Ikaros does not contribute to the upregulation of *p27* observed in these cells.

In conclusion, these data demonstrate an important role for Ikaros in T cell development and leukemogenesis. The cooperation observed between Ikaros and RBP-J proposes that Ikaros can alter Notch target gene expression, thereby facilitating T cell development. It also suggests that loss of Ikaros in leukemogenesis results in a more severe phenotype, as Ikaros could, at least in

part, regulate aberrant Notch activity observed in Notch induced leukemia. In our model, aberrant Notch expression contributes to the leukemic phenotype, however, it is not the cause. Loss of Ikaros alone results in a proliferative defect that cannot be corrected by loss of ICN expression.

Chapter V.

Summary

Cancer development results from cellular events that disrupt signaling, differentiation, apoptosis, and/or proliferation. Disruption of genes classified as oncogenes and tumor suppressors is a common event in cancer as these genes encode regulators that maintain normal cellular function. Disruption of their function can accelerate onset of cancer. Our lab studies Ikaros, a lymphocytic differentiation regulator that has the properties of a tumor suppressor. Ikaros is a hematopoietic specific zinc finger DNA binding protein that has been linked to control of gene expression. It carries out this function as a component of chromatin remodeling complexes, which serve to regulate the conformation of DNA, thereby facilitating or preventing gene expression.

To examine Ikaros as a tumor suppressor for T cells, we utilized an ex vivo system to restore Ikaros activity to an Ikaros null leukemia line. This T cell line, JE131, was generated from the thymus of an Ikaros null mouse with T cell leukemia. A retroviral transduction system was used to express Ikaros in these cells. Restoration of Ikaros has dramatic effects on growth rate and cell cycle progression, reducing growth and arresting the cells in G0/G1. In addition, a potential target of Ikaros regulation has been identified. Upon reintroduction of Ikaros, JE131 cells increase expression of p27Kip1 (p27), a cell cycle regulator. JE131 cells where Ikaros has been restored also initiate a T cell development program of gene expression. JE131 cells expressing Ikaros upregulate markers of DN to DP transition in T cell development, including

CD4, CD8, TCR and CD69. JE131 cells also show a global increase in acetylation of histone H3 upon reintroduction of Ikaros.

In pursuit of a transcriptional regulator of *p27* that may be involved in Ikaros mediated upregulation of *p27*, we examined hairy enhancer of split 1, or Hes1. Hes1 is a basic helix-loop-helix transcription factor that has been shown to be important for development in multiple lineages. *Hes1* expression is high in JE131 cells, but rapidly decreases upon restoration of Ikaros expression. Chromatin immunoprecipitation studies show that H3 acetylation decreases at the *Hes1* locus upon Ikaros reintroduction and Ikaros itself binds directly to the *Hes1* promoter. Interestingly, Hes1 is a Notch target gene. Another canonical Notch target gene, Deltex1, was examined and similar results were found. Recent data have linked loss of Ikaros and Notch gain of function as cooperating mutations in leukemogenesis. Our studies establish a mechanism for this cooperation, through Ikaros regulation of Notch target genes. Loss of Ikaros, however, is essential for the leukemic phenotype observed in JE131 cells. The cleaved form of Notch1, intracellular notch (ICN), is expressed aberrantly in the JE131 Ikaros null T cell line. However, addition of a γ -secretase inhibitor, which prevents cleavage of the Notch1 receptor to generate ICN, fails to potently inhibit growth. This demonstrates that loss of Ikaros alone, not expression of a Notch oncogene, is required for the aberrant growth observed in Ikaros null cells. These data suggest that Ikaros functions as a tumor suppressor in part through regulation of Notch target gene expression.

The changes that occur in Ikaros null cells transduced with Ikaros demonstrate the important role that Ikaros plays in the regulation of T cell growth control and development. It also defines Ikaros as a tumor suppressor.

References

1. Knudson, A.G., Jr. 1971. Mutation and cancer: statistical study of retinoblastoma. *Proc Natl Acad Sci U S A* 68:820-823.
2. Tomlinson, I.P., R. Roylance, and R.S. Houlston. 2001. Two hits revisited again. *J Med Genet* 38:81-85.
3. Kopnin, B.P. 2000. Targets of oncogenes and tumor suppressors: key for understanding basic mechanisms of carcinogenesis. *Biochemistry (Mosc)* 65:2-27.
4. Kozma, L., I. Kiss, S. Szakall, and I. Ember. 1994. Investigation of c-myc oncogene amplification in colorectal cancer. *Cancer Lett* 81:165-169.
5. Amati, B., T.D. Littlewood, G.I. Evan, and H. Land. 1993. The c-Myc protein induces cell cycle progression and apoptosis through dimerization with Max. *Embo J* 12:5083-5087.
6. Freytag, S.O., and T.J. Geddes. 1992. Reciprocal regulation of adipogenesis by Myc and C/EBP alpha. *Science* 256:379-382.
7. Soussi, T., and P. May. 1996. Structural aspects of the p53 protein in relation to gene evolution: a second look. *J Mol Biol* 260:623-637.
8. el-Deiry, W.S., T. Tokino, V.E. Velculescu, D.B. Levy, R. Parsons, J.M. Trent, D. Lin, W.E. Mercer, K.W. Kinzler, and B. Vogelstein. 1993. WAF1, a potential mediator of p53 tumor suppression. *Cell* 75:817-825.
9. Diller, L., J. Kassel, C.E. Nelson, M.A. Gryka, G. Litwak, M. Gebhardt, B. Bressac, M. Ozturk, S.J. Baker, B. Vogelstein, and et al. 1990. p53 functions as a cell cycle control protein in osteosarcomas. *Mol Cell Biol* 10:5772-5781.
10. Mercer, W.E., M.T. Shields, M. Amin, G.J. Sauve, E. Appella, J.W. Romano, and S.J. Ullrich. 1990. Negative growth regulation in a glioblastoma tumor cell line that conditionally expresses human wild-type p53. *Proc Natl Acad Sci U S A* 87:6166-6170.
11. el-Deiry, W.S., J.W. Harper, P.M. O'Connor, V.E. Velculescu, C.E. Canman, J. Jackman, J.A. Pietsenpol, M. Burrell, D.E. Hill, Y. Wang, and et al. 1994. WAF1/CIP1 is induced in p53-mediated G1 arrest and apoptosis. *Cancer Res* 54:1169-1174.
12. Yonish-Rouach, E., D. Resnitzky, J. Lotem, L. Sachs, A. Kimchi, and M. Oren. 1991. Wild-type p53 induces apoptosis of myeloid leukaemic cells that is inhibited by interleukin-6. *Nature* 352:345-347.
13. Miyashita, T., M. Harigai, M. Hanada, and J.C. Reed. 1994. Identification of a p53-dependent negative response element in the bcl-2 gene. *Cancer Res* 54:3131-3135.

14. Rizzo, M.G., A. Zepparoni, B. Cristofanelli, R. Scardigli, M. Crescenzi, G. Blandino, S. Giuliacci, S. Ferrari, S. Soddu, and A. Sacchi. 1998. Wt-p53 action in human leukaemia cell lines corresponding to different stages of differentiation. *Br J Cancer* 77:1429-1438.
15. Shaulsky, G., N. Goldfinger, A. Peled, and V. Rotter. 1991. Involvement of wild-type p53 protein in the cell cycle requires nuclear localization. *Cell Growth Differ* 2:661-667.
16. Dey, B.R., V.P. Sukhatme, A.B. Roberts, M.B. Sporn, F.J. Rauscher, 3rd, and S.J. Kim. 1994. Repression of the transforming growth factor-beta 1 gene by the Wilms' tumor suppressor WT1 gene product. *Mol Endocrinol* 8:595-602.
17. Hosono, S., I. Gross, M.A. English, K.M. Hajra, E.R. Fearon, and J.D. Licht. 2000. E-cadherin is a WT1 target gene. *J Biol Chem* 275:10943-10953.
18. Loeb, D.M., D. Korz, M. Katsnelson, E.A. Burwell, A.D. Friedman, and S. Sukumar. 2002. Cyclin E is a target of WT1 transcriptional repression. *J Biol Chem* 277:19627-19632.
19. Haber, D.A., S. Park, S. Maheswaran, C. Englert, G.G. Re, D.J. Hazen-Martin, D.A. Sens, and A.J. Garvin. 1993. WT1-mediated growth suppression of Wilms tumor cells expressing a WT1 splicing variant. *Science* 262:2057-2059.
20. Werner, H., Z. Shen-Orr, F.J. Rauscher, 3rd, J.F. Morris, C.T. Roberts, Jr., and D. LeRoith. 1995. Inhibition of cellular proliferation by the Wilms' tumor suppressor WT1 is associated with suppression of insulin-like growth factor I receptor gene expression. *Mol Cell Biol* 15:3516-3522.
21. Ellisen, L.W., N. Carlesso, T. Cheng, D.T. Scadden, and D.A. Haber. 2001. The Wilms tumor suppressor WT1 directs stage-specific quiescence and differentiation of human hematopoietic progenitor cells. *Embo J* 20:1897-1909.
22. Bergmann, L., C. Miething, U. Maurer, J. Brieger, T. Karakas, E. Weidmann, and D. Hoelzer. 1997. High levels of Wilms' tumor gene (wt1) mRNA in acute myeloid leukemias are associated with a worse long-term outcome. *Blood* 90:1217-1225.
23. Mrozek, K., K. Heinonen, and C.D. Bloomfield. 2001. Clinical importance of cytogenetics in acute myeloid leukaemia. *Best Pract Res Clin Haematol* 14:19-47.
24. Georgopoulos, K., D.D. Moore, and B. Derfler. 1992. Ikaros, an early lymphoid-specific transcription factor and a putative mediator for T cell commitment. *Science* 258:808-812.
25. Molnar, A., and K. Georgopoulos. 1994. The Ikaros gene encodes a family of functionally diverse zinc finger DNA-binding proteins. *Mol Cell Biol* 14:8292-8303.
26. Sun, L., A. Liu, and K. Georgopoulos. 1996. Zinc finger-mediated protein interactions modulate Ikaros activity, a molecular control of lymphocyte development. *Embo J* 15:5358-5369.

27. Miller, J., A.D. McLachlan, and A. Klug. 1985. Repetitive zinc-binding domains in the protein transcription factor IIIA from *Xenopus* oocytes. *Embo J* 4:1609-1614.
28. Hahm, K., P. Ernst, K. Lo, G.S. Kim, C. Turck, and S.T. Smale. 1994. The lymphoid transcription factor LyF-1 is encoded by specific, alternatively spliced mRNAs derived from the Ikaros gene. *Mol Cell Biol* 14:7111-7123.
29. Sun, L., N. Heerema, L. Crotty, X. Wu, C. Navara, A. Vassilev, M. Sensel, G.H. Reaman, and F.M. Uckun. 1999. Expression of dominant-negative and mutant isoforms of the antileukemic transcription factor Ikaros in infant acute lymphoblastic leukemia. *Proceedings of the National Academy of Sciences of the United States of America* 96:680-685.
30. Tonnelle, C., B. Calmels, C. Maroc, J. Gabert, and C. Chabannon. 2002. Ikaros gene expression and leukemia. *Leuk Lymphoma* 43:29-35.
31. Tucker, S.N., H.K. Jessup, H. Fujii, and C.B. Wilson. 2002. Enforced expression of the Ikaros isoform IK5 decreases the numbers of extrathymic intraepithelial lymphocytes and natural killer 1.1+ T cells. *Blood* 99:513-519.
32. Molnar, A., P. Wu, D.A. Largespada, A. Vortkamp, S. Scherer, N.G. Copeland, N.A. Jenkins, G. Bruns, and K. Georgopoulos. 1996. The Ikaros gene encodes a family of lymphocyte-restricted zinc finger DNA binding proteins, highly conserved in human and mouse. *J Immunol* 156:585-592.
33. Wang, J.H., A. Nichogiannopoulou, L. Wu, L. Sun, A.H. Sharpe, M. Bigby, and K. Georgopoulos. 1996. Selective defects in the development of the fetal and adult lymphoid system in mice with an Ikaros null mutation. *Immunity* 5:537-549.
34. Winandy, S., P. Wu, and K. Georgopoulos. 1995. A dominant mutation in the Ikaros gene leads to rapid development of leukemia and lymphoma. *Cell* 83:289-299.
35. Gibbons, R.J. 2005. Histone modifying and chromatin remodelling enzymes in cancer and dysplastic syndromes. *Hum Mol Genet* 14 Spec No 1:R85-92.
36. Johnson, C.A. 2000. Chromatin modification and disease. *J Med Genet* 37:905-915.
37. Kim, J., S. Sif, B. Jones, A. Jackson, J. Koipally, E. Heller, S. Winandy, A. Viel, A. Sawyer, T. Ikeda, R. Kingston, and K. Georgopoulos. 1999. Ikaros DNA-binding proteins direct formation of chromatin remodeling complexes in lymphocytes. *Immunity* 10:345-355.
38. Koipally, J., A. Renold, J. Kim, and K. Georgopoulos. 1999. Repression by Ikaros and Aiolos is mediated through histone deacetylase complexes. *Embo J* 18:3090-3100.
39. Tong, J.K., C.A. Hassig, G.R. Schnitzler, R.E. Kingston, and S.L. Schreiber. 1998. Chromatin deacetylation by an ATP-dependent nucleosome remodelling complex. *Nature* 395:917-921.

40. Zhang, Y., G. LeRoy, H.P. Seelig, W.S. Lane, and D. Reinberg. 1998. The dermatomyositis-specific autoantigen Mi2 is a component of a complex containing histone deacetylase and nucleosome remodeling activities. *Cell* 95:279-289.
41. Woodage, T., M.A. Basrai, A.D. Baxevanis, P. Hieter, and F.S. Collins. 1997. Characterization of the CHD family of proteins. *Proc Natl Acad Sci U S A* 94:11472-11477.
42. Koipally, J., and K. Georgopoulos. 2002. A molecular dissection of the repression circuitry of Ikaros. *J Biol Chem* 277:15015-15021.
43. Muchardt, C., and M. Yaniv. 1993. A human homologue of *Saccharomyces cerevisiae* SNF2/SWI2 and *Drosophila* brm genes potentiates transcriptional activation by the glucocorticoid receptor. *Embo J* 12:4279-4290.
44. Klochendler-Yeivin, A., C. Muchardt, and M. Yaniv. 2002. SWI/SNF chromatin remodeling and cancer. *Curr Opin Genet Dev* 12:73-79.
45. Schreiber-Agus, N., and R.A. DePinho. 1998. Repression by the Mad(Mxi1)-Sin3 complex. *Bioessays* 20:808-818.
46. Koipally, J., E.J. Heller, J.R. Seavitt, and K. Georgopoulos. 2002. Unconventional potentiation of gene expression by Ikaros. *J Biol Chem* 277:13007-13015.
47. Zhang, C.L., T.A. McKinsey, J.R. Lu, and E.N. Olson. 2001. Association of COOH-terminal-binding protein (CtBP) and MEF2-interacting transcription repressor (MITR) contributes to transcriptional repression of the MEF2 transcription factor. *J Biol Chem* 276:35-39.
48. Sundqvist, A., K. Sollerbrant, and C. Svensson. 1998. The carboxy-terminal region of adenovirus E1A activates transcription through targeting of a C-terminal binding protein-histone deacetylase complex. *FEBS Lett* 429:183-188.
49. Koipally, J., and K. Georgopoulos. 2000. Ikaros interactions with CtBP reveal a repression mechanism that is independent of histone deacetylase activity. *J Biol Chem* 275:19594-19602.
50. Gomez-del Arco, P., K. Maki, and K. Georgopoulos. 2004. Phosphorylation controls Ikaros's ability to negatively regulate the G(1)-S transition. *Mol Cell Biol* 24:2797-2807.
51. Jantz, D., and J.M. Berg. 2004. Reduction in DNA-binding affinity of Cys2His2 zinc finger proteins by linker phosphorylation. *Proc Natl Acad Sci U S A* 101:7589-7593.
52. Gomez-del Arco, P., J. Koipally, and K. Georgopoulos. 2005. Ikaros SUMOylation: Switching Out of Repression. *Mol. Cell. Biol.* 25:2688-2697.

53. Pui, J.C., D. Allman, L. Xu, S. DeRocco, F.G. Karnell, S. Bakkour, J.Y. Lee, T. Kadesch, R.R. Hardy, J.C. Aster, and W.S. Pear. 1999. Notch1 expression in early lymphopoiesis influences B versus T lineage determination. *Immunity* 11:299-308.
54. Godfrey, D.I., J. Kennedy, T. Suda, and A. Zlotnik. 1993. A developmental pathway involving four phenotypically and functionally distinct subsets of CD3-CD4-CD8- triple-negative adult mouse thymocytes defined by CD44 and CD25 expression. *J Immunol* 150:4244-4252.
55. Tsukiyama, T., N. Ishida, M. Shirane, Y.A. Minamishima, S. Hatakeyama, M. Kitagawa, K. Nakayama, and K. Nakayama. 2001. Down-regulation of p27Kip1 expression is required for development and function of T cells. *J Immunol* 166:304-312.
56. Robey, E., and B.J. Fowlkes. 1994. Selective events in T cell development. *Annu Rev Immunol* 12:675-705.
57. Guidos, C.J. 1996. Positive selection of CD4+ and CD8+ T cells. *Curr Opin Immunol* 8:225-232.
58. Gebuhr, T.C., G.I. Kovalev, S. Bultman, V. Godfrey, L. Su, and T. Magnuson. 2003. The role of Brg1, a catalytic subunit of mammalian chromatin-remodeling complexes, in T cell development. *J Exp Med* 198:1937-1949.
59. Chi, T.H., M. Wan, P.P. Lee, K. Akashi, D. Metzger, P. Chambon, C.B. Wilson, and G.R. Crabtree. 2003. Sequential roles of Brg, the ATPase subunit of BAF chromatin remodeling complexes, in thymocyte development. *Immunity* 19:169-182.
60. Williams, C.J., T. Naito, P.G. Arco, J.R. Seavitt, S.M. Cashman, B. De Souza, X. Qi, P. Keables, U.H. Von Andrian, and K. Georgopoulos. 2004. The chromatin remodeler Mi-2beta is required for CD4 expression and T cell development. *Immunity* 20:719-733.
61. Sawada, S., and D.R. Littman. 1993. A heterodimer of HEB and an E12-related protein interacts with the CD4 enhancer and regulates its activity in T-cell lines. *Mol Cell Biol* 13:5620-5628.
62. Winandy, S., L. Wu, J.H. Wang, and K. Georgopoulos. 1999. Pre-T cell receptor (TCR) and TCR-controlled checkpoints in T cell differentiation are set by Ikaros. *J Exp Med* 190:1039-1048.
63. Avitahl, N., S. Winandy, C. Friedrich, B. Jones, Y. Ge, and K. Georgopoulos. 1999. Ikaros sets thresholds for T cell activation and regulates chromosome propagation. *Immunity* 10:333-343.
64. Urban, J.A., and S. Winandy. 2004. Ikaros Null Mice Display Defects in T Cell Selection and CD4 versus CD8 Lineage Decisions. *J Immunol* 173:4470-4478.

65. Georgopoulos, K., M. Bigby, J.H. Wang, A. Molnar, P. Wu, S. Winandy, and A. Sharpe. 1994. The Ikaros gene is required for the development of all lymphoid lineages. *Cell* 79:143-156.
66. Harker, N., T. Naito, M. Cortes, A. Hostert, S. Hirschberg, M. Tolaini, K. Roderick, K. Georgopoulos, and D. Kioussis. 2002. The CD8alpha gene locus is regulated by the Ikaros family of proteins. *Mol Cell* 10:1403-1415.
67. Naito, T., P. Gomez-Del Arco, C.J. Williams, and K. Georgopoulos. 2007. Antagonistic interactions between Ikaros and the chromatin remodeler Mi-2beta determine silencer activity and Cd4 gene expression. *Immunity* 27:723-734.
68. Ernst, P., K. Hahm, and S.T. Smale. 1993. Both LyF-1 and an Ets protein interact with a critical promoter element in the murine terminal transferase gene. *Mol Cell Biol* 13:2982-2992.
69. Kallenbach, S., N. Doyen, M. Fanton d'Andon, and F. Rougeon. 1992. Three lymphoid-specific factors account for all junctional diversity characteristic of somatic assembly of T-cell receptor and immunoglobulin genes. *Proc Natl Acad Sci U S A* 89:2799-2803.
70. Trinh, L.A., R. Ferrini, B.S. Cobb, A.S. Weinmann, K. Hahm, P. Ernst, I.P. Garraway, M. Merckenschlager, and S.T. Smale. 2001. Down-regulation of TDT transcription in CD4(+)CD8(+) thymocytes by Ikaros proteins in direct competition with an Ets activator. *Genes Dev* 15:1817-1832.
71. Johansen, K.M., R.G. Fehon, and S. Artavanis-Tsakonas. 1989. The notch gene product is a glycoprotein expressed on the cell surface of both epidermal and neuronal precursor cells during Drosophila development. *J Cell Biol* 109:2427-2440.
72. Ellisen, L.W., J. Bird, D.C. West, A.L. Soreng, T.C. Reynolds, S.D. Smith, and J. Sklar. 1991. TAN-1, the human homolog of the Drosophila notch gene, is broken by chromosomal translocations in T lymphoblastic neoplasms. *Cell* 66:649-661.
73. Radtke, F., A. Wilson, G. Stark, M. Bauer, J. van Meerwijk, H.R. MacDonald, and M. Aguet. 1999. Deficient T cell fate specification in mice with an induced inactivation of Notch1. *Immunity* 10:547-558.
74. Huang, E.Y., A.M. Gallegos, S.M. Richards, S.M. Lehar, and M.J. Bevan. 2003. Surface expression of Notch1 on thymocytes: correlation with the double-negative to double-positive transition. *J Immunol* 171:2296-2304.
75. Baron, M. 2003. An overview of the Notch signalling pathway. *Semin Cell Dev Biol* 14:113-119.
76. Felli, M.P., M. Maroder, T.A. Mitsiadis, A.F. Campese, D. Bellavia, A. Vacca, R.S. Mann, L. Frati, U. Lendahl, A. Gulino, and I. Screpanti. 1999. Expression pattern of notch1, 2 and 3 and Jagged1 and 2 in lymphoid and stromal thymus components: distinct ligand-receptor interactions in intrathymic T cell development. *Int Immunol* 11:1017-1025.

77. Schroeter, E.H., J.A. Kisslinger, and R. Kopan. 1998. Notch-1 signalling requires ligand-induced proteolytic release of intracellular domain. *Nature* 393:382-386.
78. De Strooper, B., W. Annaert, P. Cupers, P. Saftig, K. Craessaerts, J.S. Mumm, E.H. Schroeter, V. Schrijvers, M.S. Wolfe, W.J. Ray, A. Goate, and R. Kopan. 1999. A presenilin-1-dependent γ -secretase-like protease mediates release of Notch intracellular domain. *Nature* 398:518-522.
79. Hsieh, J.J., T. Henkel, P. Salmon, E. Robey, M.G. Peterson, and S.D. Hayward. 1996. Truncated mammalian Notch1 activates CBF1/RBPJk-repressed genes by a mechanism resembling that of Epstein-Barr virus EBNA2. *Mol Cell Biol* 16:952-959.
80. Wu, L., J.C. Aster, S.C. Blacklow, R. Lake, S. Artavanis-Tsakonas, and J.D. Griffin. 2000. MAML1, a human homologue of Drosophila Mastermind, is a transcriptional co-activator for NOTCH receptors. *Nat Genet* 26:484-489.
81. Kao, H.Y., P. Ordentlich, N. Koyano-Nakagawa, Z. Tang, M. Downes, C.R. Kintner, R.M. Evans, and T. Kadesch. 1998. A histone deacetylase corepressor complex regulates the Notch signal transduction pathway. *Genes Dev* 12:2269-2277.
82. Oswald, F., M. Winkler, Y. Cao, K. Astrahantseff, S. Bourteele, W. Knochel, and T. Borggreffe. 2005. RBP-Jkappa/SHARP recruits CtIP/CtBP corepressors to silence Notch target genes. *Mol Cell Biol* 25:10379-10390.
83. Tun, T., Y. Hamaguchi, N. Matsunami, T. Furukawa, T. Honjo, and M. Kawaichi. 1994. Recognition sequence of a highly conserved DNA binding protein RBP-J kappa. *Nucleic Acids Res* 22:965-971.
84. David-Fung, E.S., M.A. Yui, M. Morales, H. Wang, T. Taghon, R.A. Diamond, and E.V. Rothenberg. 2006. Progression of regulatory gene expression states in fetal and adult pro-T-cell development. *Immunol Rev* 209:212-236.
85. Yamamoto, N., S. Yamamoto, F. Inagaki, M. Kawaichi, A. Fukamizu, N. Kishi, K. Matsuno, K. Nakamura, G. Weinmaster, H. Okano, and M. Nakafuku. 2001. Role of Deltex-1 as a transcriptional regulator downstream of the Notch receptor. *J Biol Chem* 276:45031-45040.
86. Tomita, K., M. Hattori, E. Nakamura, S. Nakanishi, N. Minato, and R. Kageyama. 1999. The bHLH gene Hes1 is essential for expansion of early T cell precursors. *Genes Dev* 13:1203-1210.
87. Weng, A.P., A.A. Ferrando, W. Lee, J.P. Morris, L.B. Silverman, C. Sanchez-Irizarry, S.C. Blacklow, A.T. Look, and J.C. Aster. 2004. Activating Mutations of NOTCH1 in Human T Cell Acute Lymphoblastic Leukemia. *Science* 306:269-271.

88. Malecki, M.J., C. Sanchez-Irizarry, J.L. Mitchell, G. Histen, M.L. Xu, J.C. Aster, and S.C. Blacklow. 2006. Leukemia-associated mutations within the NOTCH1 heterodimerization domain fall into at least two distinct mechanistic classes. *Mol Cell Biol* 26:4642-4651.
89. Beverly, L.J., and A.J. Capobianco. 2003. Perturbation of Ikaros isoform selection by MLV integration is a cooperative event in Notch1C-induced T cell leukemogenesis. *Cancer Cell* 3:551-564.
90. Lopez-Nieva, P., J. Santos, and J. Fernandez-Piqueras. 2004. Defective expression of Notch1 and Notch2 in connection to alterations of c-Myc and Ikaros in {gamma}-radiation-induced mouse thymic lymphomas. *Carcinogenesis* 25:1299-1304.
91. Zweidler-McKay, P.A., and W.S. Pear. 2004. Notch and T cell malignancy. *Semin Cancer Biol* 14:329-340.
92. Horton, R.M., Z.L. Cai, S.N. Ho, and L.R. Pease. 1990. Gene splicing by overlap extension: tailor-made genes using the polymerase chain reaction. *Biotechniques* 8:528-535.
93. Ito, Y. 2004. Oncogenic potential of the RUNX gene family: 'overview'. *Oncogene* 23:4198-4208.
94. Lutterbach, B., and S.W. Hiebert. 2000. Role of the transcription factor AML-1 in acute leukemia and hematopoietic differentiation. *Gene* 245:223-235.
95. Rubnitz, J.E., and A.T. Look. 1998. Molecular genetics of childhood leukemias. *J Pediatr Hematol Oncol* 20:1-11.
96. O'Neil, J., and A.T. Look. 2007. Mechanisms of transcription factor deregulation in lymphoid cell transformation. *Oncogene* 26:6838-6849.
97. Ishimaru, F., N. Avitahl, H. Dansako, K. Matsuo, K. Fujii, N. Sezaki, H. Nakayama, T. Yano, S. Fukuda, K. Imajoh, M. Takeuchi, A. Miyata, M. Hara, M. Yasukawa, I. Takahashi, H. Taguchi, K. Matsue, S. Nakao, Y. Niho, K. Takenaka, K. Shinagawa, K. Ikeda, K. Niiya, and M. Harada. 2000. Decreases in Ikaros activity correlate with blast crisis in patients with chronic myelogenous leukemia. *Cancer Research* 60:4062-4065.
98. Ishimaru, F., Y. Katayama, K. Nakase, N. Sezaki, K. Takenaka, K. Shinagawa, K. Ikeda, K. Niiya, M. Harada, and S. Olivero. 2000. Detection of different Ikaros isoforms in human leukaemias using real-time quantitative polymerase chain reaction. *Experimental Hematology* 28:1232-1238.
99. Morimoto, A., S. Ikushima, N. Kakazu, S. Hada, Y. Tabata, T. Yagi, T. Inaba, S. Hibi, T. Sugimoto, S. Imashuku, and M. Takanashi. 2002. Expression of the Ikaros gene family in childhood acute lymphoblastic leukaemia. *Leukemia* 16:2302-2308.

100. Hunter, S., L.J. Bernard, K. Payne-Wilks, C.L. Roland, L.C. Elam, Z. Feng, R.S. Levine, and K.J. Payne. 2002. Cutting edge: predominant expression of a novel Ikaros isoform in normal human hemopoiesis. *Preventive Medicine* 34:536-545.
101. Grignani, F., T. Kinsella, A. Mencarelli, M. Valtieri, D. Riganelli, F. Grignani, L. Lanfrancone, C. Peschle, G.P. Nolan, and P.G. Pelicci. 1998. High-efficiency gene transfer and selection of human hematopoietic progenitor cells with a hybrid EBV/retroviral vector expressing the green fluorescence protein. *Cancer Res* 58:14-19.
102. Kinsella, T.M., and G.P. Nolan. 1996. Episomal vectors rapidly and stably produce high-titer recombinant retrovirus. *Hum Gene Ther* 7:1405-1413.
103. Koopman, G., C.P. Reutelingsperger, G.A. Kuijten, R.M. Keehnen, S.T. Pals, and M.H. van Oers. 1994. Annexin V for flow cytometric detection of phosphatidylserine expression on B cells undergoing apoptosis. *Blood* 84:1415-1420.
104. Polyak, K., M.H. Lee, H. Erdjument-Bromage, A. Koff, J.M. Roberts, P. Tempst, and J. Massague. 1994. Cloning of p27Kip1, a cyclin-dependent kinase inhibitor and a potential mediator of extracellular antimitogenic signals. *Cell* 78:59-66.
105. Toyoshima, H., and T. Hunter. 1994. p27, a novel inhibitor of G1 cyclin-Cdk protein kinase activity, is related to p21. *Cell* 78:67-74.
106. Kim, W.Y., and N.E. Sharpless. 2006. The regulation of INK4/ARF in cancer and aging. *Cell* 127:265-275.
107. Shaulsky, G., N. Goldfinger, A. Peled, and V. Rotter. 1991. Involvement of wild-type p53 in pre-B-cell differentiation in vitro. *Proc Natl Acad Sci U S A* 88:8982-8986.
108. Luo, X.N., J.C. Reddy, P.L. Yeyati, A.H. Idris, S. Hosono, D.A. Haber, J.D. Licht, and G.F. Atweh. 1995. The tumor suppressor gene WT1 inhibits ras-mediated transformation. *Oncogene* 11:743-750.
109. Pagano, M., S.W. Tam, A.M. Theodoras, P. Beer-Romero, G. Del Sal, V. Chau, P.R. Yew, G.F. Draetta, and M. Rolfe. 1995. Role of the ubiquitin-proteasome pathway in regulating abundance of the cyclin-dependent kinase inhibitor p27. *Science* 269:682-685.
110. Hirano, M., H. Kanaide, and K. Hirano. 2007. Rac1-dependent transcriptional up-regulation of p27Kip1 by homophilic cell-cell contact in vascular endothelial cells. *Biochim Biophys Acta* 1773:1500-1510.
111. Chassot, A.A., L. Turchi, T. Virolle, G. Fitsialos, M. Batoz, M. Deckert, V. Dulic, G. Meneguzzi, R. Busca, and G. Ponzio. 2007. Id3 is a novel regulator of p27kip1 mRNA in early G1 phase and is required for cell-cycle progression. *Oncogene* 26:5772-5783.
112. Dijkers, P.F., R.H. Medema, C. Pals, L. Banerji, N.S. Thomas, E.W. Lam, B.M. Burgering, J.A. Raaijmakers, J.W. Lammers, L. Koenderman, and P.J. Coffey. 2000.

- Forkhead transcription factor FKHR-L1 modulates cytokine-dependent transcriptional regulation of p27(KIP1). *Mol Cell Biol* 20:9138-9148.
113. Soddu, S., G. Blandino, R. Scardigli, S. Coen, A. Marchetti, M.G. Rizzo, G. Bossi, L. Cimino, M. Crescenzi, and A. Sacchi. 1996. Interference with p53 protein inhibits hematopoietic and muscle differentiation. *J Cell Biol* 134:193-204.
 114. Cheng, T., and D.T. Scadden. 2002. Cell cycle entry of hematopoietic stem and progenitor cells controlled by distinct cyclin-dependent kinase inhibitors. *Int J Hematol* 75:460-465.
 115. Taniguchi, T., H. Endo, N. Chikatsu, K. Uchamaru, S. Asano, T. Fujita, T. Nakahata, and T. Motokura. 1999. Expression of p21(Cip1/Waf1/Sdi1) and p27(Kip1) cyclin-dependent kinase inhibitors during human hematopoiesis. *Blood* 93:4167-4178.
 116. Yaroslavskiy, B., S. Watkins, A.D. Donnenberg, T.J. Patton, and R.A. Steinman. 1999. Subcellular and cell-cycle expression profiles of CDK-inhibitors in normal differentiating myeloid cells. *Blood* 93:2907-2917.
 117. Takebayashi, K., Y. Sasai, Y. Sakai, T. Watanabe, S. Nakanishi, and R. Kageyama. 1994. Structure, chromosomal locus, and promoter analysis of the gene encoding the mouse helix-loop-helix factor HES-1. Negative autoregulation through the multiple N box elements. *J. Biol. Chem.* 269:5150-5156.
 118. Sasai, Y., R. Kageyama, Y. Tagawa, R. Shigemoto, and S. Nakanishi. 1992. Two mammalian helix-loop-helix factors structurally related to Drosophila hairy and Enhancer of split. *Genes Dev* 6:2620-2634.
 119. Tomita, K., M. Ishibashi, K. Nakahara, S.L. Ang, S. Nakanishi, F. Guillemot, and R. Kageyama. 1996. Mammalian hairy and Enhancer of split homolog 1 regulates differentiation of retinal neurons and is essential for eye morphogenesis. *Neuron* 16:723-734.
 120. Kunisato, A., S. Chiba, E. Nakagami-Yamaguchi, K. Kumano, T. Saito, S. Masuda, T. Yamaguchi, M. Osawa, R. Kageyama, H. Nakauchi, M. Nishikawa, and H. Hirai. 2003. HES-1 preserves purified hematopoietic stem cells ex vivo and accumulates side population cells in vivo. *Blood* 101:1777-1783.
 121. Kaneta, M., M. Osawa, K. Sudo, H. Nakauchi, A.G. Farr, and Y. Takahama. 2000. A role for pref-1 and HES-1 in thymocyte development. *J Immunol* 164:256-264.
 122. Choi, J.W., C. Pampeno, S. Vukmanovic, and D. Meruelo. 2002. Characterization of the transcriptional expression of Notch-1 signaling pathway members, Deltex and HES-1, in developing mouse thymocytes. *Dev Comp Immunol* 26:575-588.
 123. Kim, H.K., and G. Siu. 1998. The notch pathway intermediate HES-1 silences CD4 gene expression. *Mol Cell Biol* 18:7166-7175.

124. Murata, K., M. Hattori, N. Hirai, Y. Shinozuka, H. Hirata, R. Kageyama, T. Sakai, and N. Minato. 2005. Hes1 Directly Controls Cell Proliferation through the Transcriptional Repression of p27Kip1. *Mol. Cell. Biol.* 25:4262-4271.
125. Jarriault, S., C. Brou, F. Logeat, E.H. Schroeter, R. Kopan, and A. Israel. 1995. Signalling downstream of activated mammalian Notch. *Nature* 377:355-358.
126. Dumortier, A., R. Jeannet, P. Kirstetter, E. Kleinmann, M. Sellars, N.R. dos Santos, C. Thibault, J. Barths, J. Ghysdael, J.A. Punt, P. Kastner, and S. Chan. 2006. Notch Activation Is an Early and Critical Event during T-Cell Leukemogenesis in Ikaros-Deficient Mice. *Mol. Cell. Biol.* 26:209-220.
127. Georgopoulos, K. 1997. Transcription factors required for lymphoid lineage commitment. *Curr Opin Immunol* 9:222-227.
128. Allen, R.D., III, H.K. Kim, S.D. Sarafova, and G. Siu. 2001. Negative Regulation of CD4 Gene Expression by a HES-1-c-Myb Complex. *Mol. Cell. Biol.* 21:3071-3082.
129. Jarriault, S., O. Le Bail, E. Hirsinger, O. Pourquie, F. Logeat, C.F. Strong, C. Brou, N.G. Seidah, and A. Israel. 1998. Delta-1 Activation of Notch-1 Signaling Results in HES-1 Transactivation. *Mol. Cell. Biol.* 18:7423-7431.
130. Morohashi, Y., T. Kan, Y. Tominari, H. Fuwa, Y. Okamura, N. Watanabe, C. Sato, H. Natsugari, T. Fukuyama, T. Iwatsubo, and T. Tomita. 2006. C-terminal fragment of presenilin is the molecular target of a dipeptidic gamma-secretase-specific inhibitor DAPT (N-[N-(3,5-difluorophenacetyl)-L-alanyl]-S-phenylglycine t-butyl ester). *J Biol Chem* 281:14670-14676.
131. O'Neil, J., J. Calvo, K. McKenna, V. Krishnamoorthy, J.C. Aster, C.H. Bassing, F.W. Alt, M. Kelliher, and A.T. Look. 2006. Activating Notch1 mutations in mouse models of T-ALL. *Blood* 107:781-785.
132. Ho, S.N., H.D. Hunt, R.M. Horton, J.K. Pullen, and L.R. Pease. 1989. Site-directed mutagenesis by overlap extension using the polymerase chain reaction. *Gene* 77:51-59.
133. Fryer, C.J., J.B. White, and K.A. Jones. 2004. Mastermind recruits CycC:CDK8 to phosphorylate the Notch ICD and coordinate activation with turnover. *Mol Cell* 16:509-520.
134. Kageyama, R., and T. Ohtsuka. 1999. The Notch-Hes pathway in mammalian neural development. *Cell research* 9:179-188.
135. Deftos, M.L., E. Huang, E.W. Ojala, K.A. Forbush, and M.J. Bevan. 2000. Notch1 signaling promotes the maturation of CD4 and CD8 SP thymocytes. *Immunity* 13:73-84.
136. Camos, M., and D. Colomer. 2006. Molecular biology in acute leukemia. *Clin Transl Oncol* 8:550-559.

137. Hruban, R.H., M. Goggins, and S.E. Kern. 1999. Molecular genetics and related developments in pancreatic cancer. *Curr Opin Gastroenterol* 15:404.
138. Pons, M., and M. Quintanilla. 2006. Molecular biology of malignant melanoma and other cutaneous tumors. *Clin Transl Oncol* 8:466-474.
139. Shattuck-Brandt, R.L., and R.N. Dubois. 1999. The molecular basis of colorectal carcinogenesis. *Curr Opin Gastroenterol* 15:3.
140. Beverly, L.J., and A.J. Capobianco. 2004. Targeting promiscuous signaling pathways in cancer: another Notch in the bedpost. *Trends Mol Med*. 10:591-598.
141. Ong, C.T., H.T. Cheng, L.W. Chang, T. Ohtsuka, R. Kageyama, G.D. Stormo, and R. Kopan. 2006. Target selectivity of vertebrate notch proteins. Collaboration between discrete domains and CSL-binding site architecture determines activation probability. *J Biol Chem* 281:5106-5119.
142. Sun, L., P.A. Goodman, C.M. Wood, M.L. Crotty, M. Sensel, H. Sather, C. Navara, J. Nachman, P.G. Steinherz, P.S. Gaynon, N. Seibel, A. Vassilev, B.D. Juran, G.H. Reaman, and F.M. Uckun. 1999. Expression of aberrantly spliced oncogenic ikaros isoforms in childhood acute lymphoblastic leukemia. *J Clin Oncol* 17:3753-3766.
143. Pear, W.S., and J.C. Aster. 2004. T cell acute lymphoblastic leukemia/lymphoma: a human cancer commonly associated with aberrant NOTCH1 signaling. *Curr Opin in Hem* 16:426-433.
144. Taniuchi, I., M. Osato, T. Egawa, M.J. Sunshine, S.C. Bae, T. Komori, Y. Ito, and D.R. Littman. 2002. Differential requirements for Runx proteins in CD4 repression and epigenetic silencing during T lymphocyte development. *Cell* 111:621-633.
145. Taniuchi, I., M.J. Sunshine, R. Festenstein, and D.R. Littman. 2002. Evidence for distinct CD4 silencer functions at different stages of thymocyte differentiation. *Mol Cell* 10:1083-1096.
146. Taniuchi, I., and D.R. Littman. 2004. Epigenetic gene silencing by Runx proteins. *Oncogene* 23:4341-4345.